In this study, we have newly constructed a series of site-specific point mutants of the HIV-1 (NL clone) *vif* gene encoding 192 aa, and examined their biological (multi- and single-cycle replication) and biochemical (immunoprecipitation/Western blotting) characteristics. Our results here have indicated that N-terminal aa (nos. 21, 32, 38, 40 and 43) and central aa (nos. 76 and 79) in Vif are critical for association with A3G/F and for their exclusion from virions, respectively. We also have showed that aa no. 69 in Vif is important for binding and exclusion of A3G/F.

2. Materials and methods

2.1. Plasmid construction

Twenty-six proviral *vif*-mutant clones of HIV-1 were newly constructed from wild-type (WT) pNL4-3 [12] by the Quik-Change site-directed mutagenesis kit (Stratagene) as previously described [13]. Oligonucleotides used to introduce mutations into pNL4-3 are shown in Table 1. Construction and characterization of the mutants designated C114A, F115A, R132A and C133A have been previously described [14]. As a negative control clone (ΔVif), pNL-Nd [14] was used. A Flag-tagged human A3G-expression vector has been described previously [10]. Construction of Flag-tagged human A3F-expression vector was performed as follows. Human A3F was amplified by RT–PCR using mRNA from a lymphocyte cell line H9 with forward (5′-GCT CTA GAA TGA ATC ACT TCA GAA ACA CAG-3′) and reverse (5′-ACG CGT CGA CCT CGA GAA TCT CCT GCA GCT TGC-3′) primers containing *Xba*I and *Sal*I sites, respectively. The reactions were 95 °C for 1 min, 63 °C for 1 min, 72 °C for 2.5 min for 10 cycles; 95 °C for 1 min, 65 °C for 1 min, 72 °C for 2.5 min for 20 cycles. The PCR product was then cloned into pcDNA3.1-Flag, an expression vector containing the FLAG-tag sequence (Invitrogen). Amino acid sequence of human A3F from H9 cells differed from the GenBank database (accession number AAH38808) only by a single aa (Y345D).

2.2. Cell culture, transfection, and virion preparation

293T and MAGI cells were maintained in Eagle's minimal essential medium supplemented with 10% heat-inactivated fetal bovine serum (FBS). H9 cells were cultured in RPMI1640 medium supplemented with 10% FBS. Plasmid DNA transfection into 293T cells was carried out by the calcium-phosphate co-precipitation method [12]. To make virion preparations, culture supernatants were harvested at 48 h post-transfection, filtered through 0.45-μm filters, and viral particles were concentrated by ultracentrifugation through 25% sucrose for 2 h at 80,000 × *g* using SW41 rotor as previously described [15].

2.3. Single- and multi-cycle replication assays

To determine single-cycle replication of mutants, viral samples were prepared from 293T cells co-transfected with each proviral clone and an expression vector of A3G or A3F at 48 h post-transfection. Single-cycle replication was then determined by the MAGI assay [16]. To determine growth kinetics of the mutants, viruses were prepared from 293T cells transfected with each proviral clone, and inoculated into H9 cells. Viral growth was monitored by the reverse transcriptase (RT) assay of the culture supernatants of infected H9 cells at intervals as previously described [17].

2.4. Western immunoblot analysis

Cell and virion fractions were prepared from 293T cells transfected with proviral clones, and lysed in a lysis buffer (1% Nonidet P-40, 50 mM Tris–HCl (pH 7.5), 150 mM NaCl, 1 mM EDTA and 1% protease inhibitor cocktail (Sigma)). The cell and virion lysates were then resolved on SDS–PAGE, followed by electrophoretic transfer to polyvinylidene fluoride membranes. The membranes were treated with anti-FLAG (Sigma), anti-Vif (NIH AIDS Research and References Reagent Program) or anti-p24 [15] antibody, and visualized by the ECL plus Western blotting detection system (Amersham Pharmacia Biotech Inc.).

2.5. Immunoprecipitation

Transfected 293T cells were lysed in the lysis buffer as above, mixed with anti-FLAG M2 agarose (Sigma), and incubated at 4 °C for 3 h. The reaction mixture was then washed three times with TBS buffer (50 mM Tris–HCl (pH 7.4), 150 mM NaCl) and eluted by the addition of 3× FLAG peptides (Sigma). After centrifugation, the supernatants were analyzed by immunoblotting.

3. Results

3.1. Generation and characterization of Vif mutants

To determine whether each of highly conserved aa residue in HIV-1 Vif is required for viral infectivity, we generated a series of substitution mutants from WT pNL4-3 including 26 new clones (Fig. 1). Target residues were not chosen from C-terminal 19 aa because they are unnecessary for Vif function [18]. Mutant virus stocks were prepared from transfected 293T cells, and inoculated into H9 cells non-permissive for ΔVif virus. Out of 30 mutants in Fig. 1, 12 clones (W21A, S32A, W38A, Y40A, Y69A, W79A, H108A, C114A, F115A, R132A, C133A and H139A) did not grow at all similarly with the ΔVif virus. In addition, H43A, E76A and D104A mutants displayed retarded growth kinetics compared with WT virus. The other mutant viruses were found to be similarly infectious for H9 cells with WT virus. In total, aa residues which are critically required for viral replication in non-permissive H9 cells were located at scattered sites except for the downstream region of the BC box (Fig. 1), indicating that N-terminal and central portions of Vif are important for its function. The HCCH motif and BC box in Vif have been reported to be essential for association with Cul5 and ElonginC, respectively, but not for interaction with A3G [3]. Therefore, to determine a functional domain(s) for binding to A3G, we mainly examined the property of the mutants with

Table 1
Oligonucleotides used to construct HIV-1 *vif* mutants in this study

Clones	Primers
E2A	5′-GATCATCAGGGATTATGGCAAACAGATGGCAGGTG
	5′-CACCTGCCATCTGTTTGCCATAATCCCTGATGATC
W11L	5′-GGCAGGTGATGATTGTGTTGCAAGTAGACAGGATG
	5′-CATCCTGTCTACTTGCAACACAATCATCACCTGCC
W21A	5′-GACAGGATGAGGATTAACACAGCGAAAAGATTAGTAAAACACC
	5′-GGTGTTTTACTAATCTTTTCGCTGTGTTAATCCTCATCCTGTC
L24A	5′-GAGGATTAACACATGGAAAAGAGCCGTAAAACACCATATG
	5′-CARARGGTGTTTTACGGCTCTTTTCCATGTGTTAATCCTC
H28A	5′-GGAAAAGATTAGTAAAACACGCCATGTATATTTCAAGCAAAGC
	5′-GCTTTCCTTGAAATATACATGGCGTGTTTTACTAATCTTTTCC
S32A	5′-CACCATATGTATATTGCAAGGAAAGCTAAGGACTG
	5′-CAGTCCTTAGCTTTCCTTGCAATATACATATGGTG
W38A	5′-CAAGGAAAGCTAAGGACGCGTTTTATAGACATCAC
	5′-GTGATGTCTATAAAACGCGTCCTTAGCTTTCCTTG
Y40A	5′-GCTAAGGACTGGTTTGCTAGACATCACTATGAAAG
	5′-CTTTCATAGTGATGTCTAGCAAACCAGTCCTTAGC
H43A	5′-GCTAAGGACTGGTTTTATAGACATGCCTATGAAAGTACTAATCC
	5′-GGATTAGTACTTTCATAGGCATGTCTATAAAACCAGTCCTTAGC
S53A	5′-CTAATCCAAAAATAAGTGCCGAAGTACACATCCC
	5′-GGGATGTGTACTTCGGCACTTATTTTTGGATTAG
P58A	5′-GTTCAGAAGTACACATCGCACTAGGGGATGCTAAATTAG
	5′-CTAATTTAGCATCCCCTAGTGCGATGTGTACTTCTGAAC
Y69A	5′-CTAAATTAGTAATAACAACAGCCTGGGGTCTGCATACAG
	5′-CTGTATGCAGACCCCAGGCTGTTGTTATTACTAATTTAG
E76A	5′-GGGTCTGCATACAGGAGCAAGAGACTGGCATTTGG
	5′-CCAAATGCCAGTCTCTTGCTCCTGTATGCAGACCC
W79A	5′-CAGGAGAAAGAGACGCGCATTTGGGTCAGGGAGTC
	5′-GACTCCCTGACCCAAATGCGCGTCTCTTTCTCCTG
S86A	5′-CATTTGGGTCAGGGAGTCGCCATAGAATGGAGGAAAAAG
	5′-CTTTTTCCTCCATTCTATGGCGACTCCCTGACCCAAATG
Y94A	5′-GGAGGAAAAAGAGAGCTAGCACACAAGTAGACCC
	5′-GGGTCTACTTGTGTGCTAGCTCTCTTTTTCCTCC
T96A	5′-GAAAAAGAGATATAGCGCACAAGTAGACCCTGACC
	5′-GGTCAGGGTCTACTTGTGCGCTATATCTCTTTTTC
D104A	5′-GACCCTGACCTAGCAGCCCAACTAATTCATCTGC
	5′-GCAGATGAATTAGTTGGGCTGCTAGGTCAGGGTC
H108A	5′-CCTAGCAGACCAACTAATTGCCCTGCACTATTTTGATTGTTTTTC
	5′-GAAAAACAATCAAAATAGTGCAGGGCAATTAGTTGGTCTGCTAGG
Y111A	5′-GACCAACTAATTCATCTGCACGCCTTTGATTGTTTTTCAGAATC
	5′-GATTCTGAAAAACAATCAAAGGCGTGCAGATGAATTAGTTGGTC
S118A	5′-CTATTTTGATTGTTTTTCAGAAGCCGCTATAAGAAATACC
	5′-GGTATTTCTTATAGCGGCTTCTGAAAAACAATCAAAATAG
H139A	5′-GAATATCAAGCAGGAGCTAACAAGGTAGGATCTC
	5′-GAGATCCTACCTTGTTAGCTCCTGCTTGATATTC
L148A	5′-GGTAGGATCTCTACAGTACGCGGCACTAGCAGCATTAATAAAAC
	5′-GTTTTATTAATGCTGCTAGTGCCGCGTACTGTAGAGATCCTACC
P162A	5′-CAAAACAGATAAAGCCAGCTTTGCCTAGTGTTAGG
	5′-CCTAACACTAGGCAAAGCTGGCTTTATCTGTTTTG
S165A	5′-GATAAAGCCACCTTTGCCTGCTGTTAGGAAACTGACAGAGG
	5′-CCTCTGTCAGTTTCCTAACAGCAGGCAAAGGTGGCTTTATC
E171A	5′-GTTAGGAAACTGACAGCGGACAGATGGAACAAGC
	5′-GCTTGTTCCATCTGTCCGCTGTCAGTTTCCTAAC

Nucleotides for mutations are underlined.

mutations in N-terminal half (W21A, S32A, W38A, Y40A, H43A, Y69A, E76A and W79A) in the following analyses.

3.2. N-terminal region (aa 21–43) of HIV-1 Vif is important for suppression of A3G

Next, we examined the effect of N-terminal mutations in HIV-1 Vif on the suppression of A3G activity. As clearly seen in the result of single-cycle replication assay in the presence of A3G (Fig. 2A), while growth-defective mutant clones (W21A, S32A, W38A, Y40A and H43A in Fig. 1) were unable to completely counter A3G, growth-competent positive controls (L24A and H28A) behaved like WT. The mobility-shift observed for the H28A Vif would probably be related to its structure. The leaky mutant H43A still retained the ability to suppress A3G in this assay. These data were consistent

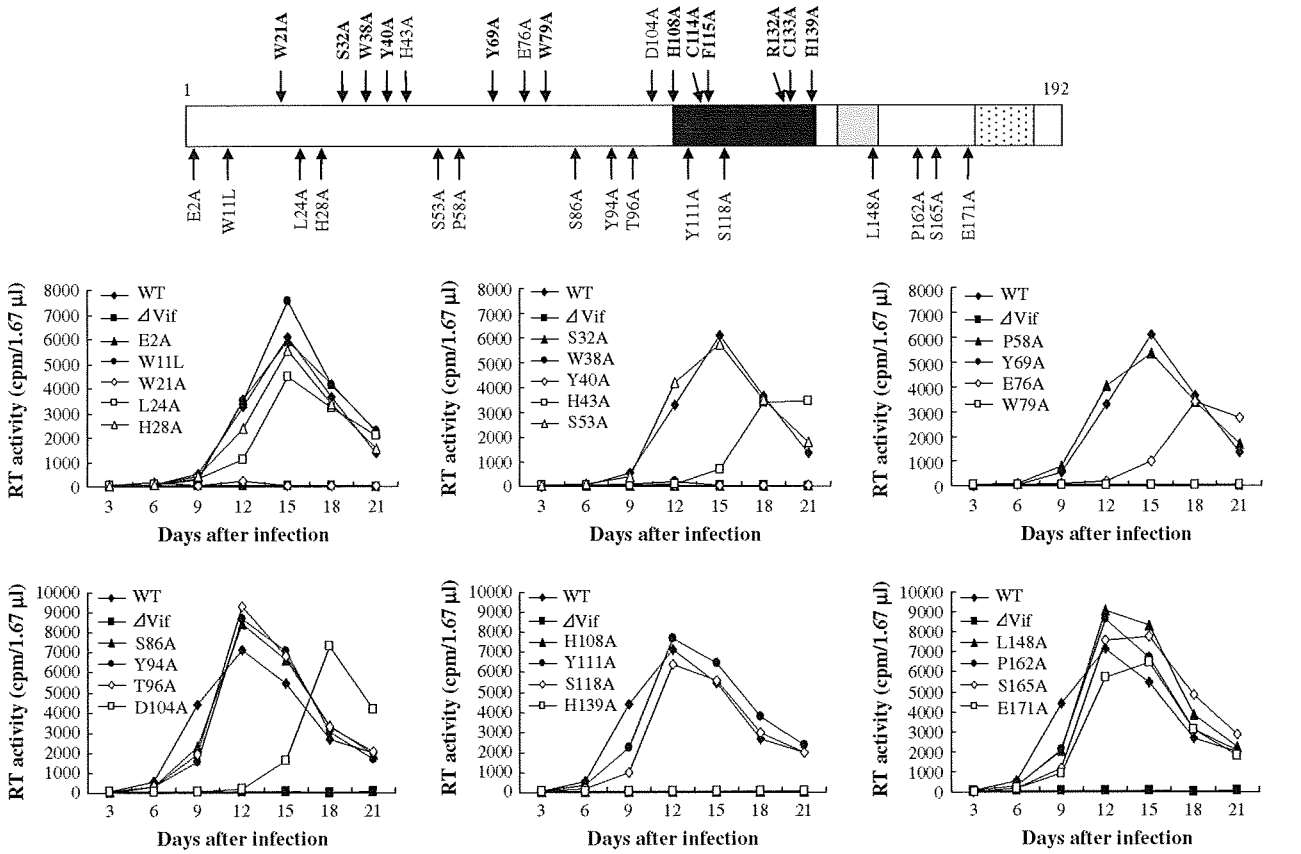

Fig. 1. Growth kinetics of various *vif* mutants in non-permissive H9 cells. H9 cells (1×10^6) were infected with an equivalent RT units (5×10^6) of cell-free viruses prepared from transfected 293T cells, and virus replication was monitored at intervals by RT production in the culture supernatants. The experiment was repeated with similar results. Locations of mutations in HIV-1 Vif (NL clone) and the mutant designations are indicated at the top. Mutants above and below the bar indicate the phenotypes of growth-defective and normal growth, respectively. Mutants in bold lines are growth-incompetent at all in H9 cells like ΔVif virus. Characterization of the mutants designated C114A, F115A, R132A and C133A has been reported previously [14]. Black, gray and dotted areas in the bar are the HCCH domain, BC-box and Basic domain, respectively.

with a conclusion that the impairment of multicycle replication of the N-terminal mutants (Fig. 1) is due to their inability to suppress A3G activity. We therefore analyzed the potentials of these mutants to control the level of A3G in virus-producing cells and in virions. As shown in Fig. 2B, WT Vif reduced somewhat the level of A3G in cells compared with the mutants, and no A3G was detected in WT virions. In contrast, none of the mutants examined here effectively excluded A3G from virions. Interaction of various Vif proteins with A3G was evaluated by co-immunoprecipitation analysis, as shown in Fig. 2C. A mutant control H108A and WT was associated with A3G but any of the other mutants was not. These data strongly suggest that the N-terminal region in Vif is required for its binding to A3G.

3.3. Glu76 and Trp79 of HIV-1 Vif are important for suppression of A3F but not for that of A3G

We further examined the effect of central region mutations (aa 69–79) in Vif on the suppression of A3G activity. As shown in Fig. 3A, although the three mutants studied here were all growth-defective in H9 cells (Y69A, E76A and W79A in Fig. 1), only the Y69A was unable to suppress A3G activity showing single-cycle replication similar to that of ΔVif clone. Thus, the expression level of A3G in virus-producing cells was monitored for the mutants (Fig. 3B). WT Vif reduced the expression of A3G relative to that by various mutants as described above. Among the mutants, only W79A was noticed to slightly reduce A3G expression. Interaction of the mutant proteins with A3G was then evaluated by the co-immunoprecipitation assay as described above. As shown in Fig. 3C, while Y69A did not bind to A3G, E76A and W79A mutants did as efficiently as WT. When the amount of A3G in virions was monitored, interestingly, only Y69A was found to be defective for exclusion of A3G among the three mutants (Fig. 3D). These results indicated that the growth-defective nature of E76A and W79A in H9 cells was not due to their defective anti-A3G activity. Based on this finding, we examined the ability of E76A and W79A mutants to act against A3F. As shown in Fig. 4A, single-cycle replication of the mutants in the presence of A3F was similarly inefficient with ΔVif mutant. The expression level in cells of A3F in the presence of mutant Vif proteins was similarly higher than that by WT

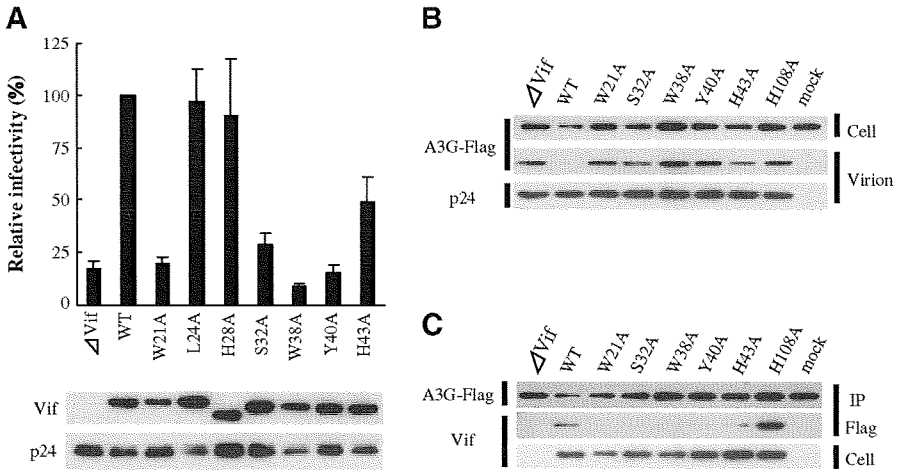

Fig. 2. Activity of various *vif* mutants (W21A, S32A, W38A, Y40A and H43A) against A3G. (A) Effect of A3G on the single-cycle replication of the mutants. Viral samples were prepared from 293T cells co-transfected with each proviral clone and an A3G-expression vector, and their infectivity was determined in MAGI cells. Expression levels of Vif and Gag-p24 as monitored by immunoblotting of lysates from transfected 293T cells are also shown at the bottom. (B) Level of A3G in virus-producing cells and in progeny virions. 293T cells were transfected with the mutant clones indicated, and cell/virion lysates for immunoblotting analysis were prepared 2 days later. H108A was used as a control (see Fig. 1). (C) Ability of WT and mutant Vif proteins to interact with A3G. Lysates of 293T cells co-transfected with each proviral clone and an A3G-expression vector were prepared, and used for immunoprecipitation (IP) of A3G-Flag by anti-Flag-M2 agarose. The interaction of various Vif proteins and A3G was then analyzed by immunoblotting using anti-Flag or anti-Vif anti-serum. Cell lysates were examined by immunoblotting analysis with anti-Vif anti-serum. The experiment in this figure was repeated with similar results.

(Fig. 4B). Interaction of mutants with A3F was then evaluated by the co-immunoprecipitation analysis as shown in Fig. 4C. Whereas WT Vif efficiently bound to A3F, Y69A and W79A (Fig. 4C, lane 5) clearly lost the ability. Even the leaky mutant E76A (Fig. 1) was very defective for binding activity. As shown in Fig. 4D, we finally analyzed the encapsidation of A3F into mutant virions. As expected, while the WT clone effectively excluded A3F from virions,

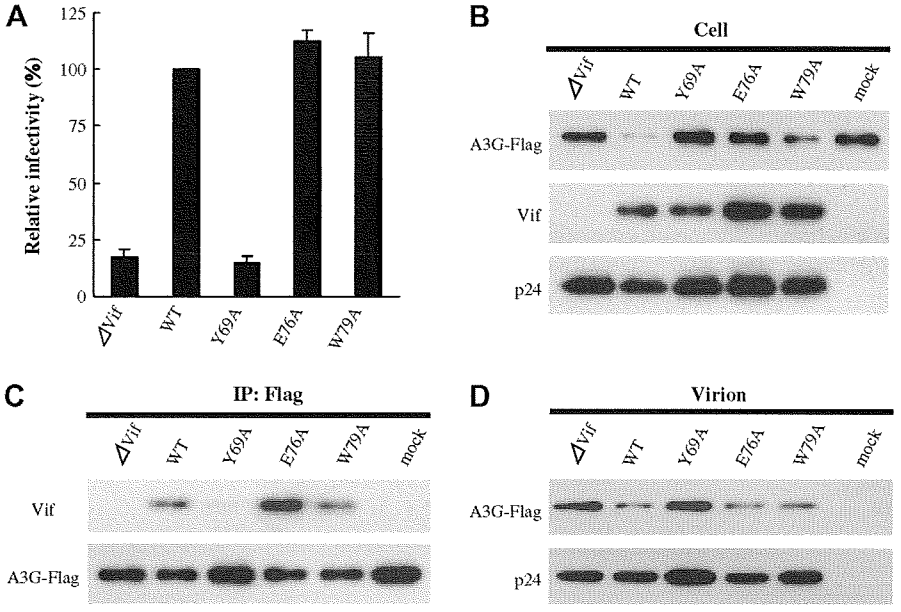

Fig. 3. Activity of *vif* mutants (Y69A, E76A and W79A) against A3G. (A) Effect of A3G on the single-cycle replication of the mutants. Viral samples were prepared from 293T cells co-transfected with each proviral clone and an A3G-expression vector, and their infectivity was determined in MAGI cells. (B) Expression level of A3G in the presence of WT or mutant Vif proteins. Samples were prepared from 293T cells transfected with each proviral clone, and analyzed by immunoblotting using antibodies indicated. (C) Ability of WT and mutant Vif proteins to interact with A3G. Lysates of 293T cells co-transfected with each proviral clone and an A3G-expression vector were prepared, and used for immunoprecipitation (IP) of A3G-Flag by anti-Flag-M2 agarose. The interaction of various Vif proteins and A3G was then analyzed by immunoblotting using anti-Flag or anti-Vif anti-serum. (D) Packaging of A3G into mutant virions. Virions prepared from 293T cells co-transfected with each proviral clone and an A3G-expression vector were examined by immunoblotting analysis using antibodies indicated. The experiment in this figure was repeated with similar results.

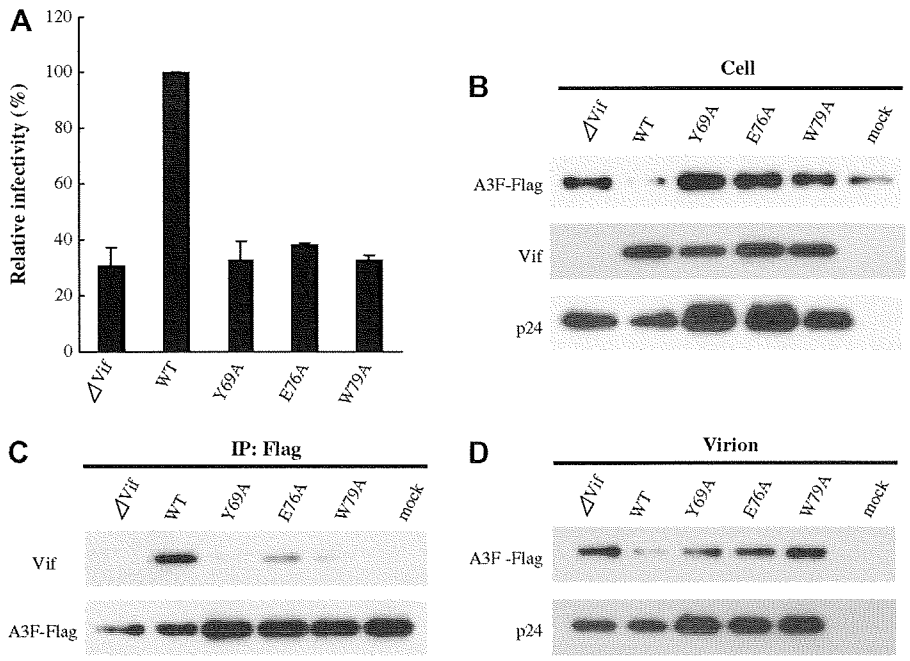

Fig. 4. Activity of *vif* mutants (Y69A, E76A and W79A) against A3F. (A) Effect of A3F on the single-cycle replication of the mutants. Viral samples were prepared from 293T cells co-transfected with each proviral clone and an A3F-expression vector, and their infectivity was determined in MAGI cells. (B) Expression level of A3F in the presence of WT or mutant Vif proteins. Samples were prepared from 293T cells transfected with each proviral clone, and analyzed by immunoblotting using antibodies indicated. (C) Ability of WT and mutant Vif proteins to interact with A3F. Lysates of 293T cells co-transfected with each proviral clone and an A3F-expression vector were prepared, and used for immunoprecipitation (IP) of A3F-Flag by anti-Flag-M2 agarose. The interaction of various Vif proteins and A3F was then analyzed by immunoblotting using anti-Flag or anti-Vif anti-serum. (D) Packaging of A3F into mutant virions. Virions prepared from 293T cells co-transfected with each proviral clone and an A3F-expression vector were examined by immunoblotting analysis using antibodies indicated. The experiment in this figure was repeated with similar results.

none of the mutants did so. These data strongly suggested that the central region in Vif is required for its binding to A3F.

4. Discussion

In this report, we have performed a systematic molecular genetic study on the A3G/F-binding function of HIV-1 Vif (NL clone). The data obtained have indicated that N-terminal aa (nos. 21, 32, 38, 40 and 43) and central aa (nos. 76 and 79) in Vif are critical for its binding to A3G/F and finally for their exclusion from virions, respectively. We also have demonstrated that aa no. 69 in Vif is important for binding and exclusion of both A3 proteins. Our results here have confirmed and significantly extended the previous reports [7–9]. Taken together, all the available data can be summarized as shown in Fig. 5. As is clear in the figure, several distinct regions in the N-terminal half of HIV-1 Vif are critical for its binding to anti-retroviral innate factors A3G/F. We showed that the N-terminal region (aa 21–38) is necessary for suppression of A3G activity through binding (Fig. 2), in addition to the conclusion previously published [8,9]. We also showed for

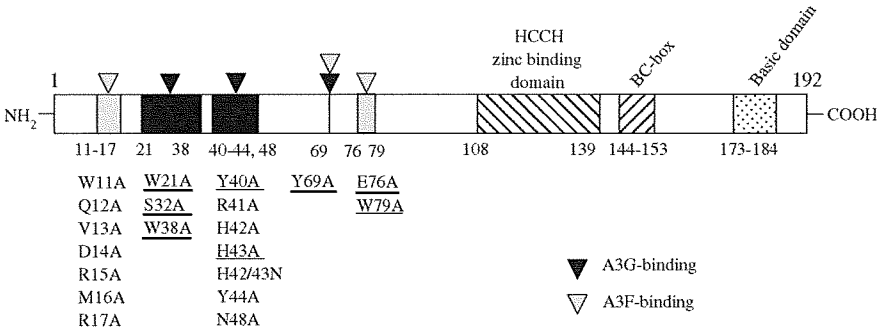

Fig. 5. Regions of HIV-1 Vif responsible for binding to A3G/F. Based on the results previously published [7–9] and presented in this study, amino acid residues critical for the binding activity of Vif are summarized. Mutations that abolish or diminish the activity are shown. The eight mutations identified in this study are underlined (bold underlines, newly identified).

the first time that the downstream region (aa 76–79) is important for suppression of A3F activity through binding (Fig. 4). Furthermore, an aa critical for suppression of both proteins was newly identified (Figs. 3 and 4).

It has been reported that negatively charged residues Asp128 and Asp130 in A3G are critical for interaction with HIV-1 Vif [19]. Our new result that aa residues 21–43 in HIV-1 Vif play a functional role for interaction with A3G is quite reasonable, considering that the region is rich in positively charged aa residues and that Vif–A3G interaction is dependent on electrostatic interaction. While Glu76 and Trp79 residues were not essential for A3G suppression (Fig. 3), they were critical for A3F suppression (Fig. 4). Of note, whereas E76A and W79A almost normally exclude A3G from virions, they degraded A3G more poorly than WT in producer cells and efficiently interacted with it (Fig. 3B and C). Inhibition of A3G incorporation into virions by HIV-1 Vif may not be a direct outcome of the Vif-mediated degradation of A3G in producer cells. It can be also claimed here that the virion-associated A3 protein is a final and fatal factor for modulation of viral infectivity in target cells. We previously reported that the region containing Tyr69 is important for formation of β-strand structure and for stable expression of Vif [13]. Similarly, a mutation of Ile9 required for β-strand structure abolished the ability of Vif to interact with A3G [20,21]. Thus, it is likely that Tyr69 is important for a proper folding of Vif molecule, and accordingly, the mutant Y69A is inactive against both of A3G and A3F.

It has been reported that some mutants of HIV-1 Vif still retain selective neutralizing activity against A3F but not A3G in a single-cycle infection [7,22]. Moreover, Asp128 of A3G is critical for recognition by HIV-1 Vif but a mutation of Glu128 in A3F does not affect the recognition [1,23]. Our data also showed that HIV-1 Vif recognizes A3G and A3F by different regions. A3G generates GG-to-AA mutations, whereas A3F causes GA-to-AA mutations [1]. GA-to-AA mutations are frequently observed in viral sequences recovered from HIV-1-infected individuals [24]. Therefore, A3F may be important for restriction of HIV-1 infection *in vivo*. In fact, our data showed that mutations of Glu76 and Trp79, which are essential for suppression of A3F activity by Vif, abolished viral multi-cycle replication in H9 cells (Fig. 1).

In this study, we demonstrated that new regions in HIV-1 Vif are critical for interaction with A3G/F. It is well anticipated that the Vif–A3G/F interaction represents a novel and important target of chemical therapy for suppression of HIV-1 replication. Understanding more fully the region in Vif required for A3G/F-binding would provide useful information on the design of antiviral drugs.

Acknowledgments

We thank Ms. Kazuko Yoshida for editorial assistance. We also thank the members of our department for their helpful discussion. This work was supported in part by a Grant-in-Aid for Scientific Research on Priority Areas (19041051) from the Ministry of Education, Culture, Sports, Science and Technology of Japan (to A.A.), and by a Health Sciences Research Grant (Research on HIV/AIDS (2007–2009)) from the Ministry of Health, Labour and Welfare of Japan (to A.A.).

References

[1] R.K. Holmes, M.H. Malim, K.N. Bishop, APOBEC-mediated viral restriction: not simply editing? Trends Biochem. Sci. 32 (2007) 118–128.
[2] A. Mehle, J. Goncalves, M. Santa-Marta, M. McPike, D. Gabuzda, Phosphorylation of a novel SOCS-box regulates assembly of the HIV-1 Vif-Cul5 complex that promotes APOBEC3G degradation, Genes Dev. 18 (2004) 2861–2866.
[3] Y. Yu, Z. Xiao, E.S. Ehrlich, X. Yu, X.F. Yu, Selective assembly of HIV-1 Vif-Cul5-ElonginB-ElonginC E3 ubiquitin ligase complex through a novel SOCS box and upstream cysteines, Genes Dev. 18 (2004) 2867–2872.
[4] K. Luo, Z. Xiao, E. Ehrlich, Y. Yu, B. Liu, S. Zheng, X.F. Yu, Primate lentiviral virion infectivity factors are substrate receptors that assemble with cullin 5-E3 ligase through a HCCH motif to suppress APOBEC3G, Proc. Natl. Acad. Sci. USA 102 (2005) 11444–11449.
[5] A. Mehle, E.R. Thomas, K.S. Rajendran, D. Gabuzda, A zinc-binding region in Vif binds Cul5 and determines cullin selection, J. Biol. Chem. 281 (2006) 17259–17265.
[6] Z. Xiao, E. Ehrlich, Y. Yu, K. Luo, T. Wang, C. Tian, X.F. Yu, Assembly of HIV-1 Vif-Cul5 E3 ubiquitin ligase through a novel zinc-binding domain-stabilized hydrophobic interface in Vif, Virology 349 (2006) 290–299.
[7] C. Tian, X. Yu, W. Zhang, T. Wang, R. Xu, X.F. Yu, Differential requirement for conserved tryptophans in human immunodeficiency virus type 1 Vif for the selective suppression of APOBEC3G and APOBEC3F, J. Virol. 80 (2006) 3112–3115.
[8] R.A. Russel, V.K. Pathak, Identification of two distinct human immunodeficiency virus type 1 Vif determinants critical for interactions with human APOBEC3G and APOBEC3F, J. Virol. 81 (2007) 8201–8210.
[9] A. Mehle, H. Wilson, C. Zhang, A.J. Brazier, M. McPike, E. Pery, D. Gabuzda, Identification of an APOBEC3G binding site in human immunodeficiency virus type 1 Vif and inhibitors of Vif-APOBEC3G binding, J. Virol. 81 (2007) 13235–13241.
[10] K. Kamada, T. Igarashi, M.A. Martin, B. Khamsri, K. Hatcho, T. Yamashita, M. Fujita, T. Uchiyama, A. Adachi, 2006. Generation of HIV-1 derivatives that productively infect macaque monkey lymphoid cells, Proc. Natl. Acad. Sci. USA 103 (2006) 16959–16964.
[11] T. Hatziioannou, M. Princiotta, M. Piatak Jr., F. Yuan, F. Zhang, J.D. Lifson, P.D. Bieniasz, Science 314 (2006) 95.
[12] A. Adachi, H.E. Gendelman, S. Koenig, T. Folks, R. Willey, A. Rabson, M.A. Martin, Production of acquired immunodeficiency syndrome-associated retrovirus in human and nonhuman cells transfected with an infectious molecular clone, J. Virol. 59 (1986) 284–291.
[13] M. Fujita, H. Akari, A. Sakurai, A. Yoshida, T. Chiba, K. Tanaka, K. Strebel, A. Adachi, Expression of HIV-1 accessory protein Vif is controlled uniquely to be low and optimal by proteasome degradation, Microbes Infect. 6 (2004) 791–798.
[14] M. Fujita, A. Sakurai, A. Yoshida, S. Matsumoto, M. Miyaura, A. Adachi, Subtle mutations in the cysteine region of HIV-1 Vif drastically alter the viral replication phenotype, Microbes Infect. 4 (2002) 621–624.
[15] H. Akari, T. Fukumori, A. Adachi, Cell-dependent requirement of human immunodeficiency virus type 1 gp41 cytoplasmic tail for Env incorporation into virions, J. Virol. 74 (2000) 4891–4893.
[16] J. Kimpton, M. Emerman, Detection of replication-competent and pseudotyped human immunodeficiency virus with a sensitive cell line on the basis of activation of an integrated beta-galactosidase gene, J. Virol. 66 (1992) 2232–2239.
[17] R.L. Willey, D.H. Smith, L.A. Lasky, T.S. Theodore, P.L. Earl, B. Moss, D.J. Capon, M.A. Martin, In vitro mutagenesis identifies a region within the envelope gene of the human immunodeficiency virus that is critical for infectivity, J. Virol. 62 (1988) 139–147.
[18] A. Sakurai, A. Jere, A. Yoshida, T. Yamada, A. Iwamoto, A. Adachi, M. Fujita, Functional analysis of HIV-1 vif genes derived from Japanese

long-term nonprogressors and progressors for AIDS, Microbes Infect. 6 (2004) 799–805.
[19] H. Huthoff, M.H. Malim, Identification of amino acid residues in APOBEC3G required for regulation by HIV-1 Vif and virion encapsidation, J. Virol. 81 (2007) 3807–3815.
[20] M.J. Wichroski, K. Ichiyama, T.M. Rana, Analysis of HIV-1 viral infectivity factor-mediated proteasome-dependent depletion of APOBEC3G: correlating function and subcellular localization, J. Biol. Chem. 280 (2005) 8387–8396.
[21] C. Pace, J. Keller, D. Nolan, I. James, S. Gaudieri, C. Moore, S. Mallal, Population level analysis of human immunodeficiency virus type 1 hypermutation and its relationship with APOBEC3G and vif genetic variation, J. Virol. 80 (2006) 9259–9269.
[22] V. Simon, V. Zennou, D. Murray, Y. Huang, D.D. Ho, P.D. Bieniasz, Natural variation in Vif: differential impact on APOBEC3G/3F and a potential role in HIV-1 diversification, PLoS Pathog. 1 (2005) e6.
[23] B. Liu, P.T. Sarkis, K. Luo, Y. Yu, X.F. Yu, Regulation of Apobec3F and human immunodeficiency virus type 1 Vif by Vif-Cul5-ElonB/C E3 ubiquitin ligase, J. Virol. 79 (2005) 9579–9587.
[24] M.T. Liddament, W.L. Brown, A.J. Schumacher, R.S. Harris, APOBEC3F properties and hypermutation preferences indicate activity against HIV-1 in vivo, Curr. Biol. 14 (2004) 1385–1391.

ELSEVIER

INSTITUT PASTEUR

Microbes and Infection 10 (2008) 1218–1222

www.elsevier.com/locate/micinf

Short communication

Replication potentials of *vif* variant viruses generated from monkey cell-tropic HIV-1 derivative clones NL-DT5/NL-DT5R

Kazuki Hatcho, Kazuya Kamada, Tomoki Yamashita, Akio Adachi, Masako Nomaguchi*

Department of Virology, Institute of Health Biosciences, The University of Tokushima Graduate School, Tokushima 770-8503, Japan

Received 30 April 2008; accepted 3 June 2008
Available online 20 June 2008

Abstract

To obtain monkey-tropic viruses that are more closely related to HIV-1 than the original NL-DT5/NL-DT5R clones, we constructed six *vif*-chimeric and two site-specific *vif*-mutant viruses, and examined their growth ability. Different from NL-DT5/NL-DT5R, these viruses did not grow in monkey cells. We monitored the capability of the mutants to antagonize monkey APOBEC3G/F by single-cycle infectivity assays. They counteracted poorly or not at all the action of the APOBEC3G/F. Our results have indicated that the native SIVmac Vif is required to overcome the species barrier against HIV-1.

Keywords: HIV-1; SIV; Vif; APOBEC3G; APOBEC3F; Species tropism

1. Introduction

Human immunodeficiency virus type 1 (HIV-1) displays a very narrow host range, infecting only humans and chimpanzees at both cellular and individual levels. In contrast, simian immunodeficiency virus isolated from rhesus monkeys (SIVmac) can grow in Asian macaques in addition to humans and chimpanzees, although it has a genomic organization similar to that of HIV-1. The distinct host range and similar genome organization of HIV-1 and SIVmac prompted us to generate HIV-1 derivative clones that efficiently grow in macaque cells and are pathogenic for macaques. By these viruses, we would be able to have an ideal animal model for basic and clinical studies on HIV-1/AIDS. Recent attempts by us and others have demonstrated that the genomic regions responsible for the species tropism of HIV-1 are located at *gag* and *vif* genes [1,2]. We have also shown that the substitution of cyclophilin A-binding loop within Gag-CA of HIV-1 with the corresponding region of SIVmac is critical for viral growth in monkey cells [1]. Whether the entire *vif* of SIVmac is essential to overcome the monkey barrier against HIV-1 remained to be determined.

In this study, we have asked whether some specific amino acids and/or domains of SIVmac Vif confer the ability on the virus to productively infect monkey cells. Towards this end, we adopted the strategy to construct *vif* chimeras and site-specific *vif*-mutants, and evaluate their potentials to grow in monkey cells. In addition, we determined the activity of variant Vif proteins against the target proteins APOBEC3G (A3G) and APOBEC3F (A3F) present in monkey cells. We demonstrate here that the whole *vif* gene of SIVmac is required for the productive infection of HIV-1 variants in monkey cells.

2. Materials and methods

2.1. Proviral molecular clones

Full-length infectious molecular clones designated pNL4-3 (HIV-1) [3], pMA239 (SIVmac) [4], pNL-DT5 (monkey cell-tropic HIV-1 derivative defective for *vpr* expression) [1], and pNL-DT5R (monkey cell-tropic HIV-1 derivative) [1] have been previously described. Various *vif*-chimeric variants (Fig. 1A) were constructed by connecting two PCR products

* Corresponding author. Tel.: +81 88 633 9232; fax: +81 88 633 7080.
E-mail address: nomaguchi@basic.med.tokushima-u.ac.jp (M. Nomaguchi).

1286-4579/$ - see front matter © 2008 Elsevier Masson SAS. All rights reserved.
doi:10.1016/j.micinf.2008.06.007

amplified from pNL-Sca [1] and pNL-ScaV [1] using the primers in Table 1, and by their insertion into pNL-DT5. To generate site-specific *vif*-mutants (Fig. 1A), Sca-pUC which carries the *vif* gene of pNL-Sca were first constructed. Mutant sequences were then amplified from Sca-pUC by the QuikChange® Site-Directed Mutagenesis Kit (Stratagene, LA Jolla, CA) using the primers in Table 1 as previously described [5,6], and the altered *vif* genes were inserted into pNL-DT5R. The *vif*-deficient clone of pNL-DT5R designated pNL-DT5R-ΔV was constructed by introducing a frame-shift mutation at *Bgl*II site.

2.2. Expression vectors of species-specific APOBEC proteins

Expression vectors of species-specific A3G have been previously described [1]. Species-specific A3F genes were cloned from cDNAs amplified from human H9 and cynomolgus monkey HSC-F cells by RT-PCR. The A3F gene was amplified with forward (GCTCTAGAATGAAGCCTCACTTCAGAAA CACAG) and reverse (ACGCGTCGACCTCGAGAATCTCC TGCAGCTTGC) primers containing embedded *Xba*I and *Sal*I sites (underlined), respectively. The reaction mixtures were heated at 95 °C for 3 min for 1 cycle; 95 °C for 1 min, 63 °C for 1 min, 72 °C for 2.5 min for 10 cycles; 95 °C for 1 min, 65 °C for 1 min, 72 °C for 2.5 min for 25 cycles; and 72 °C for 5 min for 1 cycle. The PCR products were inserted into pcDNA3.1-FLAG vector at the *Nhe*I and *Xho*I sites. Expression level of A3F proteins in transfected 293T cells were determined by Western blotting analysis using anti-FLAG antibody as previously described [1]. Because the expression level in cells of the original clone for cynomolgus monkey A3F was found to be quite low, three point mutations (as judged by the GenBank data on A3F) were corrected for high level expression.

2.3. Cell culture, transfection, and infection

A human kidney cell line 293T [7] was cultured in Eagle's minimal essential medium supplemented with 10% heat-inactivated fetal bovine serum. M8166 (human T-cell line) [4] and HSC-F (simian T-cell line) [8] cells were cultured in RPMI-1640 medium supplemented with 10% heat-inactivated fetal bovine serum. Virus stocks were prepared from 293T cells transfected with various variant clones by the calcium-phosphate coprecipitation method [3]. On day 2 post-transfection, culture supernatants were collected and stored at −80 °C until use. Infection of M8166 and HSC-F cells with viruses was performed essentially as previously described [9].

2.4. RT assay

Virion-associated RT activity was measured as previously described [10].

2.5. Single-cycle infectivity assay

To determine single-cycle infectivity of *vif* variant viruses in the presence of APOBEC proteins, we used luciferase reporter assay as previously described [11]. For this assay, we utilized VSV-G-pseudotyped viruses prepared from 293T cells co-transfected with a luciferase reporter clone and an expression vector of the species-specific APOBEC protein at a ratio of 15:1 (total 10 μg plasmids), and 0.8 μg of the VSV-G expression vector [12]. As reporters, proviral clones structurally similar to that described previously [13] were used. The culture supernatants were harvested on day 2 post-transfection, and were measured for RT activity. 293T cells (4.0×10^4) were infected with 8.0×10^3 RT units of VSV-G-pseudotyped viruses, and on day 2 post-infection, cell lysates were prepared for luciferase assay. Luciferase activity was determined by the Luciferase Assay System (Promega, Madison, WI) using Lumat LB9507 luminomeater (BERTHOLD TECHNOLOGIES GmbH & Co. KG, Bad Wildbad, Germany), and normalized by protein amount.

3. Results

3.1. Construction and characterization of vif variants in the genomic background of NL-DT5 and NL-DT5R

To generate monkey-tropic HIV-1 derivatives which are more closely related to HIV-1 than NL-DT5/NL-DT5R [1], we first constructed six NL-DT5-based *vif*-chimeric clones as shown in Fig. 1A. Viral samples were prepared from 293T cells transfected with these clones, and inoculated into HSC-F cells. No virus production was noted for any chimeras during observation period (30 days) as summarized in Fig. 1A. We, therefore, constructed new mutants from NL-DT5R (Fig. 1A) based on a recently published report [14] to obtain virus clones infections for HSC-F cells. The variants designated NL-DT5R-VSa and NL-DT5R-VSm contained the SIVagm SERQ and SIVmac PER sequences, respectively (Fig. 1A). The HIV-1 Vif containing the SERQ at 14–17 residues was shown to counteract the anti-viral effect of human and rhesus monkey A3Gs [14]. Although the SIVmac PER is the corresponding sequence of SIVagm SERQ, its functional importance was not tested yet [14]. To determine the growth ability of these NL-DT5R-based *vif* variant viruses in human and monkey cells, virus samples prepared from transfected 293T cells were inoculated into M8166 and HSC-F cells. As shown in Fig. 1B (upper), all the viruses grew to a various degree in permissive human M8166 cells as expected. In contrast, only MA239 (SIVmac) and NL-DT5R grew considerably in HSC-F cells (Fig. 1B, lower), indicating that variant Vif proteins are not functional in HSC-F cells.

3.2. Single-cycle infectivity of site-specific HIV-1 vif-mutants in the presence of APOBEC3G/F

To know whether mutant Vif proteins (Fig. 1A) can suppress the negative effect of human and monkey A3Gs, viral infectivity in the presence of A3Gs was determined by single-round replication assays. VSV-G-pseudotyped luciferase reporter viruses were prepared from transfected 293T cells

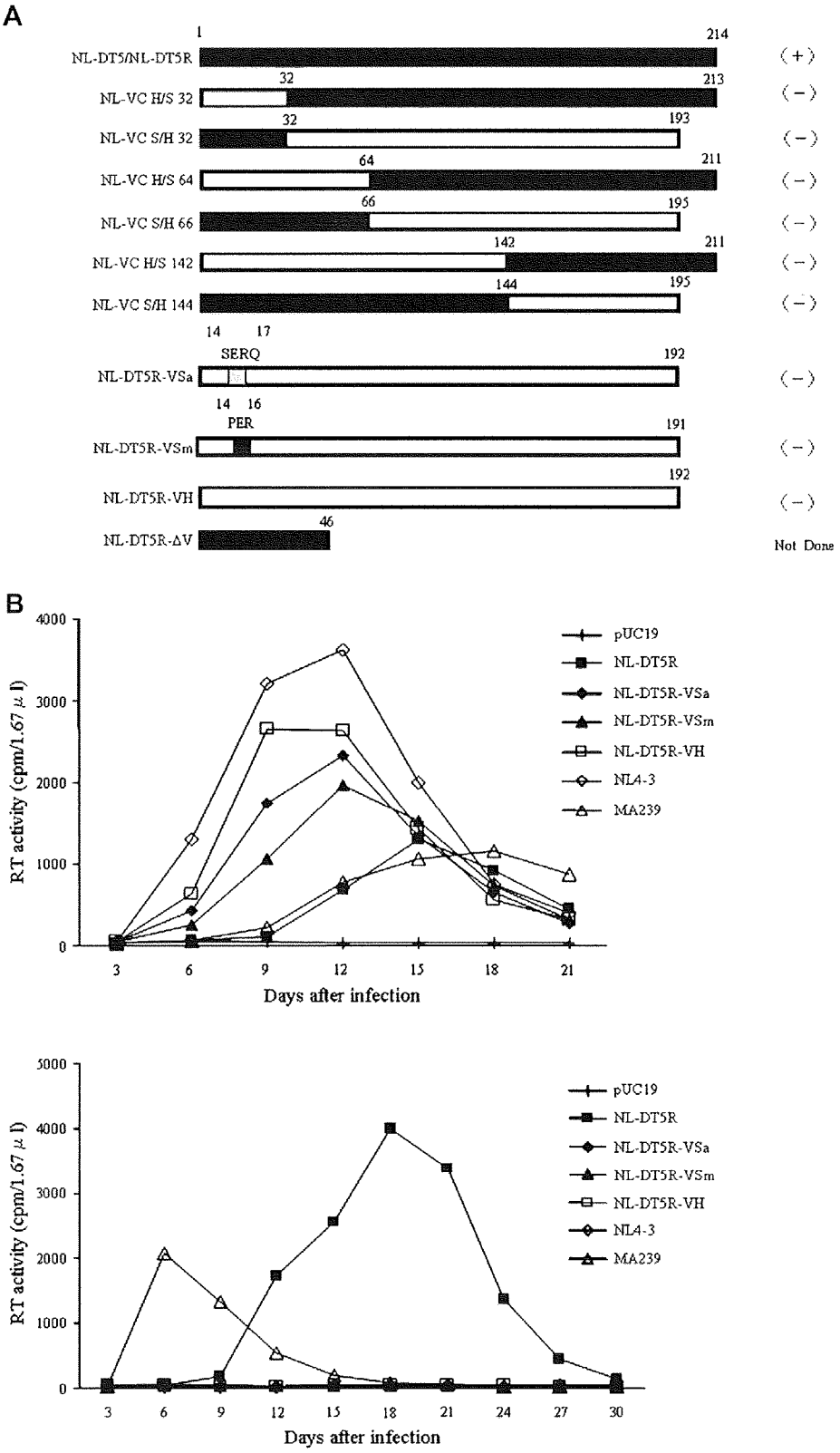

Fig. 1. Structure of variant Vif proteins and growth kinetics of variant viruses. (A) Chimeric and mutant Vif proteins derived from NL-DT and NL-DT5R. White, black and gray areas indicate the Vif sequence of HIV-1, SIVmac and SIVagm, respectively. The figures above the bars indicate nos. of amino acids. (+) and (−) on the right show positive and no viral growth in HSC-F cells, respectively. (B) Growth kinetics of various viruses in human and simian cells. Virus samples were prepared from 293T cells transfected with the indicated plasmid clones, and were inoculated into human M8166 (upper) and cynomolgus monkey HSC-F (lower) cells. M8166 (1×10^6) and HSC-F (1×10^7) cells were infected with an equal amount of viruses (1×10^6 and 1×10^7 RT units for each cell line, respectively). Viral growth was monitored at intervals by RT activity in the culture supernatants. Clones pNL4-3 (HIV-1), pMA239 (SIVmac) and pUC19 served as controls.

Table 1
Oligonucleotides used to construct *vif* variants in this study

Clone	Primer	Template
H/S 32	5′-GGGGCAGTAGTAATACAAGATAATAGTGAC	NL-Sca
	5′-GCTCTAGAAATATACATATGGTGTTTTA CTAATC	
	5′-GCTCTAGAGATCTACAAAAGGTTTGCTA TGTGCCC	NL-ScaV
	5′-ATTTCTTGCTCTCCTCTGTCGAGTAACGCC	
S/H 32	5′-GGGGCAGTAGTAATACAAGATAATAGTGAC	NL-ScaV
	5′-GCTCTAGATTTATATTTCAGATATTTTA TGAGGC	
	5′-GCTCTAGAAAAGCTAAGGACTGGTTTT ATAGAC	NL-Sca
	5′-ATTTCTTGCTCTCCTCTGTCGAGTAACGCC	
H/S 64	5′-GGGGCAGTAGTAATACAAGATAATAGTGAC	NL-Sca
	5′-TACCGCTCGAGTTTAGCATCCCCTAG TGGGATGTG	
	5′-ATCCGCTCGAGGTACAAGGGTATTGGCA TTTGAC	NL-ScaV
	5′-ATTTCTTGCTCTCCTCTGTCGAGTAACGCC	
S/H 66	5′-GGGGCAGTAGTAATACAAGATAATAGTGAC	NL-ScaV
	5′-TACCGCTCGAGATGGCTTCCTTCCTGTA GTGGG	
	5′-ATCCGCTCGAGATAACAACATATTGGG GTCTGC	NL-Sca
	5′-ATTTCTTGCTCTCCTCTGTCGAGTAACGCC	
H/S 142	5′-GGGGCAGTAGTAATACAAGATAATAGTGAC	NL-Sca
	5′-CATGGTACCTTGTTATGTCCTGCTTGAT ATTCAC	
	5′-ATGGGTACCAAGCCTACAGTACTTAGCACTG AAAG	NL-ScaV
	5′-ATTTCTTGCTCTCCTCTGTCGAGTAACGCC	
S/H144	5′-GGGGCAGTAGTAATACAAGATAATAGTGAC	NL-ScaV
	5′-CATGGTACCTGGTACTTATGAGCTCTCGGG AACC	
	5′-ATGGGTACCATCTCTACAGTACTTGGCAC TAGCAG	NL-Sca
	5′-ATTTCTTGCTCTCCTCTGTCGAGTAACGCC	
VSa	5′-GATTGTGTGGCAAGTAAGCGAGAGGCAGA TTAACACATGGAAAAG	Sca-pUC
	5′-CTTTTCCATGTGTTAATCTGCCTCTCGCTT ACTTGCCACACAATC	
VSm	5′-GATTGTGTGGCAAGTACCGGAGAGGAT TAACACATG	Sca-pUC
	5′-CATGTGTTAATCCTCTCCGGTACTTGCC ACACAATC	

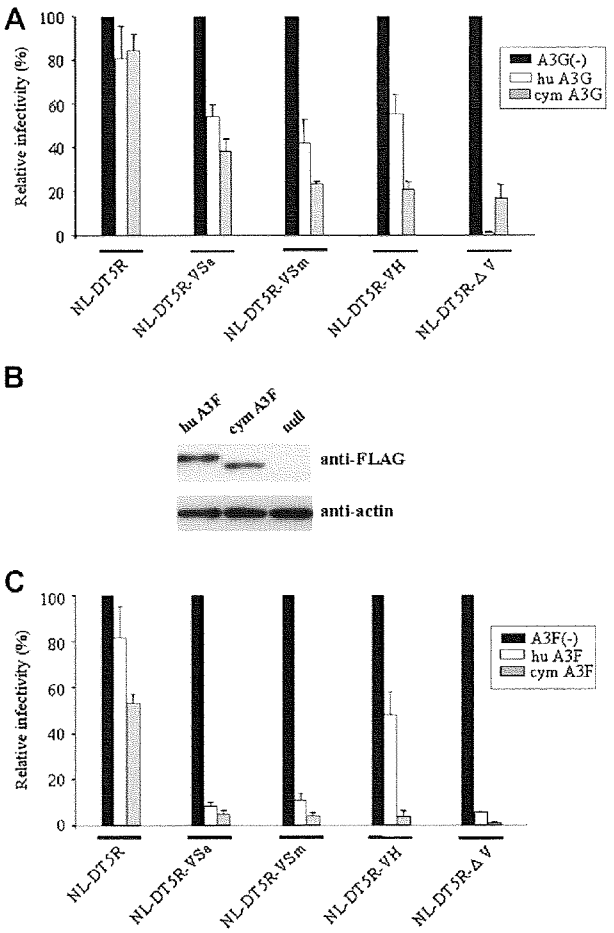

Fig. 2. Single-cycle infectivity of *vif* variants in the presence of human and monkey A3G/Fs. (A) Single-cycle infectivity of various viruses produced in the presence of human and cynomolgus monkey A3Gs (hu A3G and cym A3G, respectively). The infectivity was determined as described in Section 2. Infectivity relative to that of the virus sample prepared in the absence of A3G [A3G(−)] is shown. Viral clones used are indicated at the bottom. (B) Expression of A3Fs by newly constructed vectors as monitored by Western immunoblotting analysis. Antibodies used are indicated on the right. (C) Single-cycle infectivity of *vif* variants produced in the presence of human and monkey A3Fs. The infectivity was determined as described in Section 2. Infectivity relative to that of the virus sample prepared in the absence of A3F [A3F(−)] is shown. Viral clones used are indicated at the bottom.

in the presence or absence of A3G, and were inoculated into 293T cells. On day 2 after inoculation, intracellular luciferase activity was determined. The expression levels in cells of the A3Gs were similar on this condition [1]. As shown in Fig. 2A, all the viruses, except for a negative control NL-DT5R-ΔV, counteracted the effect of huA3G (human). While NL-DT5R-VSa containing a small portion of SIVagm Vif counteracted cymA3G (cynomolgus monkey) approximately 2-fold more effectively than NL-DT5R-VH containing HIV-1 Vif, its activity was approximately 2-fold less than that of NL-DT5R containing the entire Vif of SIVmac. These results showed that the mutant HIV-1 Vif carrying the SERQ sequence was partially active against cymA3G and that the SIVmac Vif more effectively and powerfully suppressed cymA3G activity than the mutant. On the other hand, NL-DT5R-VSm containing a small portion of SIVmac Vif suppressed huA3G activity but not considerably cymA3G activity.

To examine whether NL-DT5R and NL-DT5R-based *vif* variants counteract the effect of A3Fs, we performed single-cycle infectivity assays as above in the presence of species-specific A3Fs. A3F has been reported to be one of the APOBEC3 families and a Vif-dependent antiretroviral restriction factor like A3G [15,16]. In the first, species-specific A3F expression vectors were constructed as described in Section 2. Expression level of A3F proteins in transfected 293T cells were analyzed by immunoblotting using anti-FLAG and anti-actin antibodies as shown in Fig. 2B. Both hu and cymA3F were equally expressed in transfected 293T cells as expected. Single-cycle infectivity of various virus clones produced in 293T cells in the

presence or absence of hu and cymA3Fs was then determined. As shown in Fig. 2C, control clones NL-DT5R, NL-DT5R-VH and NL-DT5R-ΔV behaved exactly as expected. However, test samples NL-DT5R-VSa and NL-DT5R-VSm did not suppress the effect of hu and cymA3Fs at all. These results indicated that the HIV-1 Vif containing alterations at amino acid positions 14–17 was unable to counteract cymA3F activity. Furthermore, we noticed that the alteration in HIV-1 Vif also inactivated the inhibition potential against huA3F.

4. Discussion

In this study, we constructed eight HIV-1 derivatives which contain the mutated *vif* gene and examined their growth potentials to narrow down the necessary *vif* sequence of SIVmac from the genome of the prototype monkey-tropic HIV-1 designated NL-DT5/NL-DT5R (Fig. 1). However, none of them were able to grow in monkey HSC-F cells (Fig. 1). To clarify the underlying molecular mechanism for this, we evaluated the ability of mutant viruses to invalidate the activity of anti-viral APOBEC3G/F (Fig. 2). As a result, inhibitory activity against cymA3G of *vif* variant viruses was less than that of NL-DT5R. Of note, NL-DT5R-VSa containing the SERQ sequence at residues 14–17 of HIV-1 Vif counteracted cymA3G activity approximately 2-fold less effectively than NL-DT5R carrying the whole SIVmac Vif. Furthermore, none of the *vif* variant viruses counteracted cymA3F (and also huA3F) at all, strongly suggesting the possibility that A3F inhibited the replication of NL-DT5R-based *vif* variant viruses in monkey cells as well as A3G. We also noticed that NL-DT5R having the SIVmac Vif was only partially active against cymA3F as previously reported [17]. Given that SIVmac grows well in monkey cells and in monkeys, our result here suggested that the expression level of A3F in these cells might be low. In this regard, it would be interesting to quantitatively analyze various APOBEC3 proteins in natural target cells. It has been recently reported that several monkey APOBEC3 proteins such as A3B, A3F, A3G and A3H inhibit the growth of HIV-1 [17]. Taken all together, it would be critical to inhibit the activity of many of monkey APOBEC3 proteins for construction of monkey-tropic HIV-1 that grows similarly efficiently with SIVmac in monkey cells.

In sum, it is difficult or impossible to suppress the negative effect of all monkey APOBEC3 proteins active against the virus through the partial alteration of HIV-1 Vif. Therefore, chimeric virus clones containing the entire SIVmac *vif* gene, such as NL-DT5R, would be more useful monkey-tropic HIV-1 derivatives to obtain replication-competent HIV-1 that is highly pathogenic for monkeys.

Acknowledgments

We thank Ms. Kazuko Yoshida for her excellent editorial assistance. This work was supported in part by a Grant-in-Aid for Scientific Research on Priority Areas (19041051) from the Ministry of Education, Culture, Sports, Science and Technology of Japan (to A. A.), and by a Health Sciences Research Grant (Research on HIV/AIDS (2007–2009)) from the Ministry of Health, Labour and Welfare of Japan (to A. A.).

Reference

[1] K. Kamada, T. Igarashi, M.A. Martin, B. Khamsri, K. Hatcho, T. Yamashita, M. Fujita, T. Uchiyama, A. Adachi, Generation of HIV-1 derivatives that productively infect macaque monkey lymphoid cells, Proc. Natl. Acad. Sci. USA. 103 (2006) 16959–16964.

[2] T. Hatziioannou, M. Princiotta, M. Piatak Jr., F. Yuan, F. Zhang, J.D. Lifson, P.D. Bieniasz, Generation of simian-tropic HIV-1 by restriction factor evasion, Science. 314 (2006) 95.

[3] A. Adachi, H.E. Gendelman, S. Koenig, T. Folks, R. Willey, A. Rabson, M.A. Martin, Production of acquired immunodeficiency syndrome-associated retrovirus in human and nonhuman cells transfected with an infectious molecular clone, J. Virol. 59 (1986) 284–291.

[4] R. Shibata, M. Kawamura, H. Sakai, M. Hayami, A. Ishimoto, A. Adachi, Generation of a chimeric human and simian immunodeficiency virus infectious to monkey peripheral blood mononuclear cells, J. Virol. 65 (1991) 3514–3520.

[5] M. Fujita, A. Sakurai, A. Yoshida, M. Miyaura, A.H. Koyama, K. Sakai, A. Adachi, Amino acid residues 88 and 89 in the central hydrophilic region of human immunodeficiency virus type 1 Vif are critical for viral infectivity by enhancing the steady-state expression of Vif, J. Virol. 77 (2003) 1626–1632.

[6] M. Fujita, H. Akari, A. Sakurai, A. Yoshida, T. Chiba, K. Tanaka, K. Strebel, A. Adachi, Expression of HIV-1 accessory protein Vif is controlled uniquely to be low and optimal by proteasome degradation, Microbes Infect. 6 (2004) 791–798.

[7] J.S. Lebkowski, S. Clancy, M.P. Calos, Simian virus 40 replication in adenovirus-transformed human cells antagonizes gene expression, Nature. 317 (1985) 169–171.

[8] H. Akari, T. Fukumori, S. Iida, A. Adachi, Induction of apoptosis in herpesvirus saimiri-immortalized T lymphocytes by blocking interaction of CD28 with CD80/CD86, Biochem. Biophys. Res. Commun. 263 (1999) 352–356.

[9] T. Folks, S. Benn, A. Rabson, T. Theodore, M.D. Hoggan, M. Martin, M. Lightfoote, K. Sell, Characterization of a continuous T-cell line susceptible to the cytopathic effects of acquired immune deficiency syndrome (AIDS)-associated retrovirus, Proc. Natl. Acad. Sci. USA. 82 (1985) 4539–4543.

[10] R.L. Willey, D.H. Smith, L.A. Lasky, T.S. Theodore, P.L. Earl, B. Moss, D.J. Capon, M.A. Martin, In vitro mutagenesis identifies a region within the envelope gene of the human immunodeficiency virus that is critical for infectivity, J. Virol. 62 (1988) 139–147.

[11] R. Mariani, D. Chen, B. Schröfelbauer, F. Navarro, R. König, B. Bollman, C. Münk, H. Nymark-McMahon, N.R. Landau, Species-specific exclusion of APOBEC3G from HIV-1 virions by Vif, Cell. 114 (2003) 21–31.

[12] J.K. Yee, A. Miyanohara, P. LaPorte, K. Bouic, J.C. Burns, T. Friedmann, A general method for the generation of high-titer, pantropic retroviral vectors: highly efficient infection of primary hepatocytes, Proc. Natl. Acad. Sci. USA. 91 (1994) 9564–9568.

[13] R.I. Connor, B.K. Chen, S. Choe, N.R. Landau, Vpr is required for efficient replication of human immunodeficiency virus type-1 in mononuclear phagocytes, Virology. 206 (1995) 935–944.

[14] B. Schröfelbauer, T. Senger, G. Manning, N.R. Landau, Mutational alteration of human immunodeficiency virus type 1 Vif allows for functional interaction with nonhuman primate APOBEC3G, J. Virol. 80 (2006) 5984–5991.

[15] Y.H. Zheng, D. Irwin, T. Kurosu, K. Tokunaga, T. Sata, B.M. Peterlin, Human APOBEC3F is another host factor that blocks human immunodeficiency virus type 1 replication, J. Virol. 78 (2004) 6073–6076.

[16] H.L. Wiegand, B.P. Doehle, H.P. Bogerd, B.R. Cullen, A second human antiretroviral factor, APOBEC3F, is suppressed by the HIV-1 and HIV-2 Vif proteins, EMBO J. 23 (2004) 2451–2458.

[17] C.A. Virgen, T. Hatziioannou, Antiretroviral activity and Vif sensitivity of rhesus macaque APOBEC3 proteins, J. Virol. 81 (2007) 13932–13937.

ELSEVIER

INSTITUT PASTEUR

Microbes and Infection 10 (2008) 1387–1392

www.elsevier.com/locate/micinf

Short communication

Functional region mapping of HIV-2 Vpx protein

Mikako Fujita [a], Masami Otsuka [a], Masako Nomaguchi [b], Akio Adachi [b,*]

[a] *Department of Bioorganic Medicinal Chemistry, Faculty of Medical and Pharmaceutical Sciences, Kumamoto University, Kumamoto 862-0973, Japan*
[b] *Department of Virology, Institute of Health Biosciences, The University of Tokushima Graduate School, 3-18-15 Kuramoto-cho, Tokushima 770-8503, Japan*

Received 16 June 2008; accepted 6 August 2008
Available online 14 August 2008

Abstract

To determine functional regions of HIV-2 Vpx, we analyzed a series of site-specific *vpx*-mutants for their growth potentials in lymphocytic cells and compared the results with those in macrophages. We found that amino acid residues important for virus growth in lymphocytic cells, in macrophages, and in both are clustered separately in Vpx. Through generation and characterization of new *vpx*-mutants, we further demonstrated that a remarkable proline-stretch present at the C-terminus of Vpx is critical for its stable expression, thereby contributing to its functional activity. Taken together, there can be functionally distinct regions in HIV-2 Vpx.

Keywords: HIV-2; Vpx; Macrophage; Lymphocyte; Proline-stretch

1. Introduction

Viruses of human immunodeficiency virus type 2 (HIV-2) group carry a *vpx* gene that encodes virion-associated accessory protein Vpx. While Vpx is essential for virus replication in primary monocyte-derived macrophages (MDMs) [1–4], it is dispensable in primary and immortalized lymphocyte cells [3,5,6]. In these lymphocyte cultures, *vpx*-minus or -defective viruses grow to a lesser extent than wild-type (WT) virus. The mechanism underlying this cell type specificity is largely unknown. We have recently shown by extensive mutational analyses that HIV-2 Vpx is important for processes of the reverse transcription of viral RNA genome and the nuclear import of viral DNA in MDMs and lymphocytic HSC-F cells, respectively [3,4]. These findings have suggested the presence of some unidentified cellular factor(s) which interact with Vpx in a cell type dependent manner. In this study, to better understand molecular basis for cell-dependent activity of Vpx, we have performed a systemic genetic analysis by using a series of site-specific mutants of HIV-2 Vpx [4]. We show here that there are distinct and common functional regions in HIV-2 Vpx important for virus growth in two different cell types, and demonstrate that the C-terminal proline-stretch of Vpx is critical for its stable expression.

2. Materials and methods

2.1. Molecular clones

Proviral molecular clones of HIV-2 designated pGL-AN and pGL-St have been previously described [6]. Construction and characterization of proviral site-specific *vpx*-mutants (Fig. 1) also have been described previously [4]. In this study, a number of proviral mutant clones and expression vectors of the mutated Vpx proteins (Fig. 2) were newly constructed by the QuikChange site-directed mutagenesis kit (Stratagene, La Jolla, CA) as previously reported [4].

2.2. Cell culture, transfection, and infection

A human kidney cell line 293T [7] was cultured in Eagle's minimal essential medium supplemented with 10% heat-inactivated fetal bovine serum. A simian lymphocyte cell line HSC-F [8,9] was cultured in RPMI-1640 medium

* Corresponding author. Tel.: +81 88 633 7078; fax: +81 88 633 7080.
E-mail address: adachi@basic.med.tokushima-u.ac.jp (A. Adachi).

1286-4579/$ - see front matter © 2008 Elsevier Masson SAS. All rights reserved.
doi:10.1016/j.micinf.2008.08.005

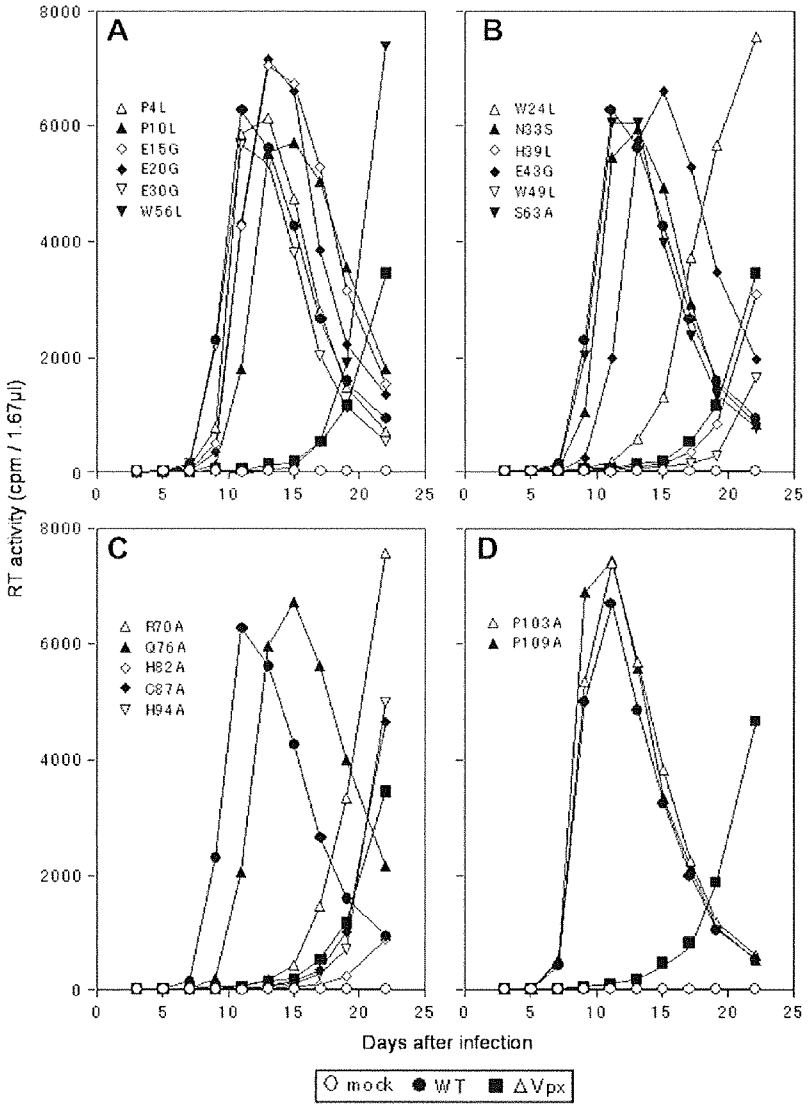

Fig. 1. Growth kinetics in HSC-F cells of various *vpx*-mutants. HSC-F cells (1×10^7) were infected with equivalent RT units of cell-free viruses (3×10^3), and viral replication was monitored at intervals by RT activity in the culture supernatants [13]. Input cell-free viruses were prepared from 293T cells transfected with 20 μg of WT pGL-AN [6] or its *vpx*-mutants. Designations of the *vpx*-mutants are indicated. Mock, pUC19; ΔVpx, pGL-St [6].

supplemented with 10% heat-inactivated fetal bovine serum. Human MDMs were prepared and cultured as previously described [3,4,10], and were 95–97% CD68-positive and completely negative for CD3. Virus stocks were prepared from 293T cells transfected with various mutant clones by the calcium-phosphate coprecipitation method [11,12]. On day 2 post-transfection, culture supernatants were collected and stored at −80 °C until use. Infection of HSC-F cells and MDMs with viruses was performed essentially as previously described [3].

2.3. Reverse transcriptase (RT) assay

Virion-associated RT activity was measured as previously described [13].

2.4. Immunoblot analysis

293T cells were transfected with various molecular clones as above, and on day 2 or 3 post-transfection, virion and cell lysates were prepared for Western immunoblot analysis with appropriate antibodies (Fig. 2) as previously described [4].

3. Results and discussion

We firstly monitored the growth property in lymphocytic cells of the site-specific *vpx*-mutants carrying a single amino acid (aa) change previously reported [4]. As described above, although Vpx is essential for virus growth in MDMs, it is not strictly required in lymphocytic cells and even the *vpx*-minus (ΔVpx) viruses can grow to a considerable level. In our

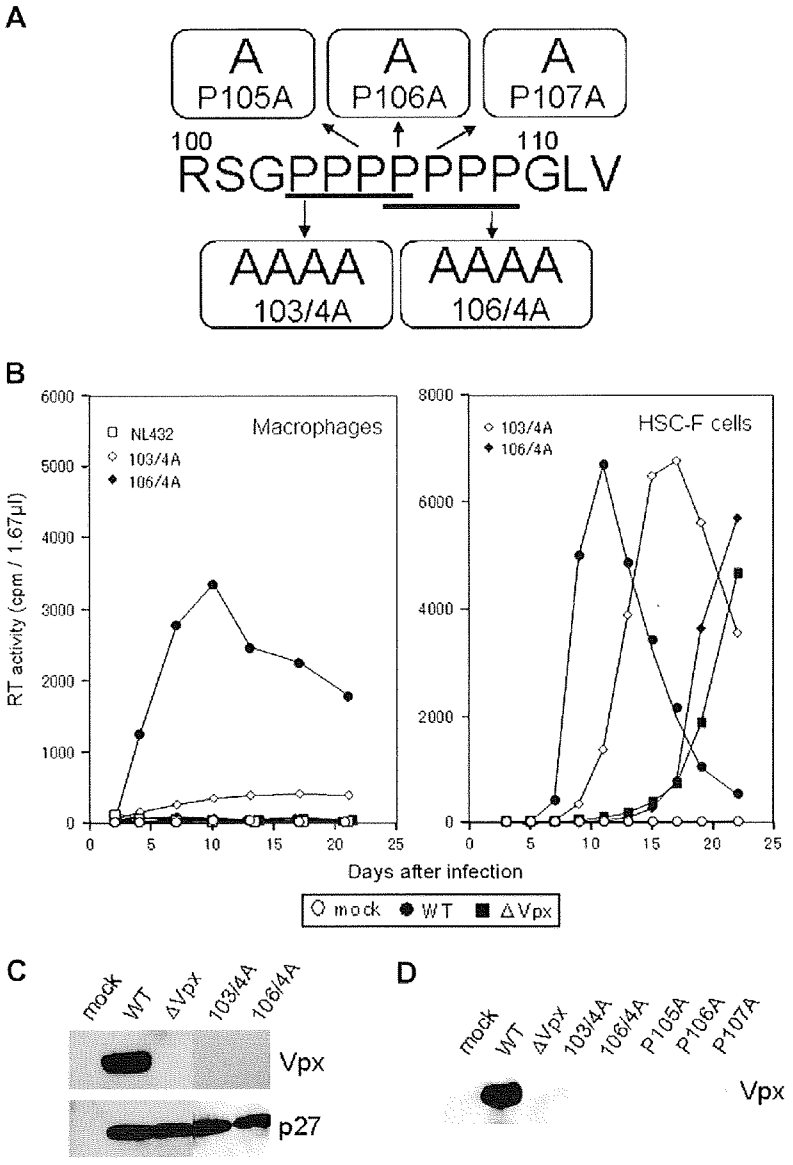

Fig. 2. Effect of proline-mutations in Vpx on viral infectivity and expression of Vpx. (A) Structure of five proline-mutants. Proviral clones were not constructed for P105A, P106A and P107A (see text). (B) Growth kinetics in MDMs and HSC-F cells of mutants 103/4A and 106/4A. Confluent MDMs in a well of 24-well tissue culture plates were infected with equivalent RT units of cell-free viruses (6×10^5) in the presence of DEAE-dextran (5 μg/ml), and viral replication was monitored at intervals by RT activity in the culture supernatants. HSC-F cells were infected with viruses and monitored for virus growth as described in the legend to Fig. 1. Input viruses were prepared from 293T cells transfected with 20 μg of WT proviral clone pGL-AN [6], its *vpx*-mutants or an HIV-1 infectious clone pNL432 [11] as a negative control. Mock, pUC19; ΔVpx, pGL-St [6]. (C) Immunoblot analysis of mutant Vpx proteins in virions. 293T cells were transfected with 20 μg of WT proviral clone pGL-AN [6] or its mutants, and on day 3 post-transfection, virion lysates were prepared as previously described [15]. The lysates were then analyzed by Western immunoblotting [10,15,21] with an HIV-2 ROD Vpx polyclonal antibody and an antiserum to SIV p27. Mock, pUC19; ΔVpx, pGL-St [6]. (D) Immunoblot analysis of mutant Vpx proteins in transfected cells. 293T cells were co-transfected with 7.5 μg of an expression vector of WT Vpx designated pME18Neo-Fvpx [21]/its *vpx*-mutants and 2.5 μg of an expression vector of luciferase (pGL3-Control Vector, Promega, Madison, WI), and on day 2 post-transfection, cell lysates were prepared as previously described [10,15,21]. The lysates normalized by luciferase activity were then analyzed by Western immunoblotting [10,15,21] with an anti-FLAG antibody (ANTI-FLAG M2 Monoclonal Antibody, Sigma-Aldrich, St. Louis, MO).

preliminary experiments, the *vpx*-minus and -mutated viruses were leaky in peripheral blood mononuclear cells (PBMCs) from different individuals, and their susceptibility to viruses was quite different depending on the donors. We, therefore, selected the HSC-F cell line [8,9] as target for virus infection to obtain consistent results. HSC-F cells were frequently and successfully used in place of PBMCs [3,14–17]. Various mutant DNA clones were transfected into 293T cells, and cell-free viruses prepared on day 2 post-transfection were inoculated into HSC-F cells. As shown in Fig. 1, all the clones including ΔVpx did grow in the cells, but to various degrees. Out of 19 mutants tested, five clones (H39L, W49L, H82A, C87A and H94A) grew similarly or even more poorly than ΔVpx, and three (W24L, W56L and R70A) showed medium

growth property between ΔVpx and WT. The infection experiments were extensively repeated and similar results were obtained.

There is a long stretch of proline residues at the C-terminal region of Vpx (Fig. 2A). It is quite conceivable that this unique sequence is important for Vpx function, and in fact, it has been reported that deletion of the C-terminal proline-rich tail in Vpx results in the complete loss of WT phenotype [2]. However, our mutants carrying mutations in this region (P103A and P109A) showed a normal or slightly affected growth phenotype [4]. We, therefore, studied the region more extensively. Two new mutant clones (103/4A and 106/4A) were constructed from WT pGL-AN by the QuikChange site-directed mutagenesis kit (Stratagene) (Fig. 2A), and examined for their properties. The mutations were confirmed by sequence analysis. Fig. 2B shows the growth kinetics of the new mutant viruses in human MDMs and HSC-F cells. As is clear in the figure, mutant 106/4A displayed the ΔVpx phenotype both in MDMs and HSC-F cells, but mutant 103/4A was less growth-defective in both cell types and grew somewhat in MDMs. These results indicated that the latter half of the proline-stretch is more important for virus growth in MDMs and HSC-F cells than the first. The infection experiments were repeated with similar results. We then examined the level of Vpx in the mutant virions. We previously reported that virions of all the site-specific mutants (19 mutants in Fig. 1) contain a comparable level of Vpx [4]. Virions were prepared from transfected 293T cells and analyzed by Western immunoblotting with a polyclonal anti-HIV-2 ROD Vpx antiserum as previously described [4,15]. As shown in Fig. 2C, mutant virions 103/4A and 106/4A clearly lacked Vpx. Thus, we then examined the intracellular expression of mutant Vpx proteins. Because detection of Vpx in cells transfected with proviral clones was quite difficult, we constructed expression vectors of mutant Vpx proteins from a FLAG-tag expression vector of WT Vpx designated pME18Neo-Fvpx as previously described [4]. In addition to expression vectors of 103/4A and 106/4A, those of P105A, P106A and P107A (Fig. 2A) were constructed for more detailed analysis. All mutations were confirmed by sequence analysis. 293T cells were transfected with these clones, and on day 2 post-transfection, cell lysates were prepared and monitored for Vpx expression by immunoblotting with an anti-FLAG antibody. An expression vector of luciferase was also transfected into the cells for normalization. As shown in Fig. 2D, no Vpx was detected for any of the mutants examined, indicating the proline residues are critical for stable expression of Vpx.

Fig. 3 summarizes the results in this study (Figs. 1 and 2) and a previous report by us [4]. As shown in panel B, many point mutations significantly affected viral infectivity in MDMs and/or HSC-F cells. The amino acids in Vpx important for virus replication in two different cell types (macrophage and lymphocyte) and in both were readily identified, and were separately clustered (regions a–d). It is also clear that most mutations did not affect significantly the expression of Vpx. The only mutations that abolish Vpx expression to an undetectable level resided in the C-terminal proline region. Based on these data, we have demonstrated here for the first time that there are several distinct regions in HIV-2 Vpx for its functionality.

We have recently reported that HIV-2 Vpx is critical for the reverse transcription of viral RNA genome and nuclear import of viral DNA in MDMs and HSC-F cells, respectively [3,4]. Also, it has been shown that the Vpx of simian immunodeficiency virus from the rhesus monkey (SIVmac) of the HIV-2 lineage is crucial for the reverse transcription process in human dendritic cells [18] and MDMs [19]. This cell type dependent or specific requirement of Vpx for early events in

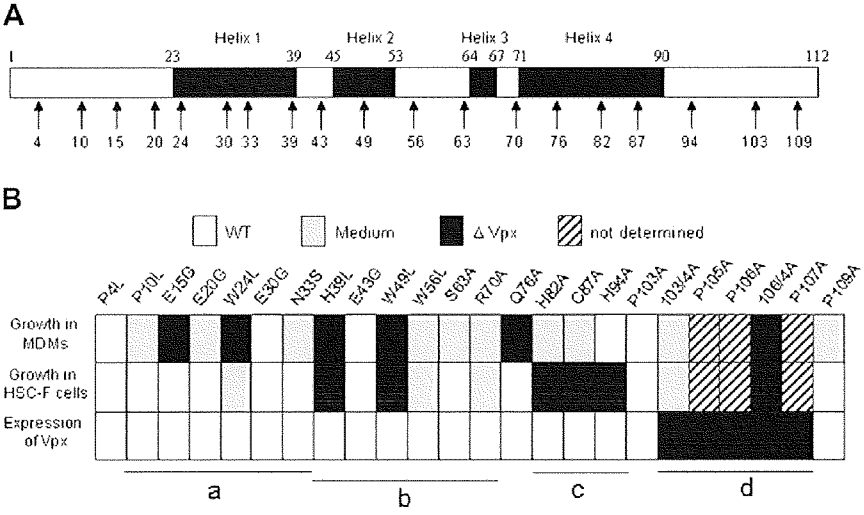

Fig. 3. Phenotype of various *vpx*-mutants. (A) Structure of HIV-2 Vpx [GL-AN clone, 112 aa (GenBank accession no. M30895)]. Black areas represent the four predicted helices [21]. Positions of point mutations (aa nos.) previously reported [4] are indicated by arrows. (B) Summary of the properties of various *vpx*-mutants. Based on our genetic studies, there can be four functional regions (a, b, c and d) in HIV-2 Vpx as shown. Region a is more important for virus growth in MDMs than that in HSC-F cells, and region c is the reverse. Region b is critical for virus growth in both cell types. Region d is essential for the expression of Vpx.

HIV-2 replication may account for the observation reported in this study, and represents a virologically very important question. Extensive molecular biological analyses of our mutants to determine precisely their defective sites in MDMs and HSC-F cells are required. Finally, to elucidate this subject, we need to identify cellular factors which are negatively or positively involved in the early process of HIV-2 replication.

Pancio et al. claimed that the C-terminal proline-rich tail of HIV-2 is necessary for nuclear localization of the viral preintegration complex in non-dividing cells [2]. Their conclusion was based on the results obtained by using a GFP-Vpx (the proline-rich tail is deleted) fusion protein and a proviral clone carrying the same deletion. They did not examine at all the expression of native mutant Vpx protein in cells and virions. Our data (Fig. 2) clearly showed that the site-specific mutations do abolish Vpx expression in cells and virions. Therefore, it is reasonable to conclude that the proline cluster at the C-terminal region of HIV-2 Vpx is essential for its expression at a normal level to maintain viral infectivity in target cells such as MDMs and HSC-F cells. As shown in Fig. 2, the mutant 106/4A displayed more attenuated growth phenotype than the mutant 103/4A. This is probably due to a difference of Vpx expression level between the two mutants, albeit undetectable. This assumption needs to be experimentally confirmed by a system more sensitive than that used here. In addition, an extensive mutational analysis of the proline region by making and characterizing proviral clones for P105A, P106A and P107A to substantiate our stability hypothesis is in progress in our laboratory.

Needless to say, it is interesting to know the mechanism by which the proline region confer stability on the entire Vpx. It has been reported that the Vpx protein associates with a complex of Cullin 4 E3 ubiquitin ligase [19,20], and this binding, in turn, may cause proteasome degradation of Vpx. The proline-rich region of Vpx may be critical for resistance to the degradation. We and others have found that the Q76A mutation abolishes viral growth ability in MDMs [4,19], and the mutant is unable to bind to the E3 ligase complex [19]. The mutant, however, grew well in HSC-F cells (Fig. 1), suggesting that the binding of Vpx to the Cullin 4 E3 ubiquitin ligase complex is important for the reverse transcription of viral RNA genome [4,19] but not for the nuclear import of viral DNA [3]. Biochemical approaches would be necessary to clarify this issue.

Acknowledgments

We thank Kazuko Yoshida for editorial assistance. We are indebted to NIH AIDS Research and References Reagent Program for an HIV-2 ROD Vpx antiserum (catalog no. 2609) and to NIBSC Centralised Facility for AIDS Reagents for an SIV p27 antiserum (repository reference ARP414). This work was supported in part by a Grant-in-Aid for Scientific Research on Priority Areas (19041051) from the Ministry of Education, Culture, Sports, Science and Technology of Japan (to A.A.).

References

[1] T.M. Fletcher, B. Brichacek, N. Sharova, M.A. Newman, G. Stivahtis, P.M. Sharp, M. Emerman, B.H. Hahn, M. Stevenson, Nuclear import and cell cycle arrest functions of the HIV-1 Vpr protein are encoded by two separate genes in HIV-2/SIV_{SM}, EMBO J. 15 (1996) 6155–6165.

[2] H.A. Pancio, N.V. Heyden, L. Ratner, The C-terminal proline-rich tail of human immunodeficiency virus type 2 Vpx is necessary for nuclear localization of the viral preintegration complex in nondividing cells, J. Virol. 74 (2000) 6162–6167.

[3] F. Ueno, H. Shiota, M. Miyaura, A. Yoshida, A. Sakurai, J. Tatsuki, A.H. Koyama, H. Akari, A. Adachi, M. Fujita, Vpx and Vpr proteins of HIV-2 up-regulate the viral infectivity by a distinct mechanism in lymphocytic cells, Microbes Infect. 5 (2003) 387–395.

[4] M. Fujita, M. Otsuka, M. Miyoshi, B. Khamsri, M. Nomaguchi, A. Adachi, Vpx is critical for the reverse transcription of human immunodeficiency virus type 2 genome in macrophages, J. Virol. 82 (2008) 7752–7756.

[5] M. Guyader, M. Emerman, L. Montagnier, K. Peden, Vpx mutants of HIV-2 are infectious in established cell lines but display a severe defect in peripheral blood lymphocytes, EMBO J. 8 (1989) 1169–1175.

[6] M. Kawamura, H. Sakai, A. Adachi, Human immunodeficiency virus Vpx is required for the early phase of replication in peripheral blood mononuclear cells, Microbiol. Immunol. 38 (1994) 871–878.

[7] J.S. Lebkowski, S. Clancy, M.P. Calos, Simian virus 40 replication in adeno-virus-transformed human cells antagonizes gene expression, Nature 317 (1985) 169–171.

[8] H. Akari, T. Fukumori, S. Iida, A. Adachi, Induction of apoptosis in *Herpesvirus saimiri*-immortalized T lymphocytes by blocking interaction of CD28 with CD80/CD86, Biochem. Biophys. Res. Commun. 263 (1999) 352–356.

[9] H. Akari, K.H. Nam, K. Mori, I. Otani, H. Shibata, A. Adachi, K. Terao, Y. Yoshikawa, Effects of SIVmac infection on peripheral blood $CD4^{+}CD8^{+}$T lymphocytes in cynomolgus macaques, Clin. Immunol. 91 (1999) 321–329.

[10] M. Fujita, A. Sakurai, A. Yoshida, M. Miyaura, A.H. Koyama, K. Sakai, A. Adachi, Amino acid residues 88 and 89 in the central hydrophilic region of human immunodefiociency virus type 1 Vif are critical for viral infectivity by enhancing the steady-state expression of Vif, J. Virol. 77 (2003) 1626–1632.

[11] A. Adachi, H.E. Gendelman, S. Koenig, T. Folks, R. Willey, A. Rabson, M.A. Martin, Production of acquired immunodeficiency syndrome-associated retrovirus in human and nonhuman cells transfected with an infectious molecular clone, J. Virol. 59 (1986) 284–291.

[12] K.B. Koh, M. Fujita, A. Adachi, Elimination of HIV-1 plasmid DNA from virus samples obtained from transfection by calcium-phosphate co-precipitation, J. Virol. Methods 90 (2000) 99–102.

[13] R.L. Willey, D.H. Smith, L.A. Lasky, T.S. Theodore, P.L. Earl, B. Moss, D.J. Capon, M.A. Martin, In vitro mutagenesis identifies a region within the envelope gene of the human immunodeficiency virus that is critical for infectivity, J. Virol. 62 (1988) 139–147.

[14] A. Adachi, M. Miyaura, A. Sakurai, A. Yoshida, A.H. Koyama, M. Fujita, Growth characteristics of SHIV without the *vpu* gene, Int. J. Mol. Med. 8 (2001) 641–644.

[15] M. Fujita, A. Yoshida, M. Miyaura, A. Sakurai, H. Akari, A.H. Koyama, A. Adachi, Cyclophilin A-independent replication of a human immunodeficiency virus type 1 isolate carrying a small portion of the simian immunodeficiency virus SIV_{MAC} *gag* capsid region, J. Virol. 75 (2001) 10527–10531.

[16] M. Fujita, A. Yoshida, A. Sakurai, J. Tatsuki, F. Ueno, H. Akari, A. Adachi, Susceptibility of HVS-immortalized lymphocytic HSC-F cells to various strains and mutants of HIV/SIV, Int. J. Mol. Med. 11 (2003) 641–644.

[17] K. Kamada, T. Igarashi, M.A. Martin, B. Khamsri, K. Hatcho, T. Yamashita, M. Fujita, T. Uchiyama, A. Adachi, Generation of HIV-1 derivatives that productively infect macaque monkey lymphoid cells, Proc. Natl. Acad. Sci. U.S.A. 103 (2006) 16959–16964.

[18] C. Goujon, L. Riviere, L. Jarrosson-Wuilleme, J. Bernaud, D. Rigal, J.-L. Darlix, A. Cimarelli, SIV_{SM}/HIV-2 Vpx proteins promote retroviral escape from a proteasome-dependent restriction pathway present in human dendritic cells, Retrovirology 4 (2007) 2.

[19] S. Srivastava, S.K. Swanson, N. Manel, L. Florens, M.P. Washburn, J. Skowronski, Lentiviral Vpx accessory factor targets VprBP/DCAF1 substrate adaptor for Cullin 4 E3 ubiquitin ligase to enable macrophage infection, PLoS Pathog. 4 (2008) e1000059.

[20] N. Sharova, Y. Wu, X. Zhu, R. Stranska, R. Kaushik, M. Sharkey, M. Stevenson, Primate lentiviral Vpx commandeers DDB1 to counteract a macrophage restriction, PLoS Pathog. 4 (2008) e1000057.

[21] B. Khamsri, F. Murao, A. Yoshida, A. Sakurai, T. Uchiyama, H. Shirai, Y. Matsuo, M. Fujita, A. Adachi, Comparative study on the structure and cytopathogenic activity of HIV Vpr/Vpx proteins, Microbes Infect. 8 (2006) 10–15.

Biochemical and Biophysical Research Communications 377 (2008) 889–893

Contents lists available at ScienceDirect

Biochemical and Biophysical Research Communications

journal homepage: www.elsevier.com/locate/ybbrc

Trans-species activation of human T cells by rhesus macaque CD1b molecules

Daisuke Morita [a,b], Kumiko Katoh [a,b], Toshiyuki Harada [c], Yoshiaki Nakagawa [c], Isamu Matsunaga [a,b], Tomoyuki Miura [d], Akio Adachi [e], Tatsuhiko Igarashi [d,*], Masahiko Sugita [a,b,*]

[a] Laboratory of Cell Regulation, Institute for Virus Research, Kyoto University, 53 Kawahara-cho, Shogoin, Sakyo-ku, Kyoto 606-8507, Japan
[b] Laboratory of Cell Regulation and Molecular Network, Graduate School of Biostudies, Kyoto University, Kyoto 606-8501, Japan
[c] Division of Applied Life Sciences, Graduate School of Agriculture, Kyoto University, Kyoto 606-8502, Japan
[d] Laboratory of Primate Model, Institute for Virus Research, Kyoto University, Kyoto 606-8507, Japan
[e] Department of Virology, Institute of Health Biosciences, The University of Tokushima Graduate School, Tokushima 770-8503, Japan

ARTICLE INFO

Article history:
Received 11 October 2008
Available online 23 October 2008

Keywords:
Rhesus macaque
CD1
Mycobacteria
Glucose monomycolate

ABSTRACT

Despite crucial importance of non-human primates as a model of human infectious diseases, group 1 CD1 genes and proteins have been poorly characterized in these species. Here, we isolated *CD1A*, *CD1B*, and *CD1C* cDNAs from rhesus macaque lymph nodes that encoded full-length CD1 proteins recognized specifically by monoclonal antibodies to human CD1a, CD1b, and CD1c molecules, respectively. The monkey group 1 CD1 isoforms contained amino acid residues and motifs known to be critical for intramolecular disulfide bond formation, N-linked glycosylation, and endosomal trafficking as in human group 1 CD1 molecules. Notably, monkey CD1b molecules were capable of presenting a mycobacterial glycolipid to human CD1b-restricted T cells, providing direct evidence for their antigen presentation function. This also detects for the first time a trans-species crossreaction mediated by group 1 CD1 molecules. Taken together, these results underscore substantial conservation of the group 1 CD1 system between humans and rhesus macaque monkeys.

Besides MHC class I- and II-restricted αβ T cells that recognize protein antigens (Ags), discrete subsets of T cells exist in humans that specifically recognize non-protein Ags in a T-cell receptor (TCR)-dependent manner. These include αβ T cells that recognize lipid, glycolipid, and lipopeptide Ags in the context of group 1 CD1 molecules (CD1a, CD1b, and CD1c) as well as $V\gamma2^+V\delta2^+$ γδ T cells that recognize pyrophosphorylated isoprenoid intermediates [1,2]. Both T cell subsets have been implicated in host defense against mycobacterial infection [3], and therefore, animal species that have evolved these T cells in addition to MHC-restricted T cells would serve as an ideal animal model of human tuberculosis. The murine model has long been studied extensively, and by taking advantage of versatile genetic manipulation and a fine array of reagents, many important aspects of host defense against tuberculosis have been demonstrated explicitly, that include a critical role for MHC-restricted T cells [4]. However, a significant difference in pathology has been noted between the two species [3], and the lack of T cells in mice that correspond to human group 1 CD1-resricted T cells and $V\gamma2^+V\delta2^+$ γδ T cells makes the animals less useful particularly in an attempt to develop a new chemical class of non-protein vaccines against tuberculosis. In contrast to mice and rats, guinea pigs exhibit pathology that is comparable, if not identical, to that in human tuberculosis, and recent studies have shown that they contain four *CD1B* genes and three *CD1C* genes [5,6]. Nevertheless, CD1a-restricted T cells as well as CD1d-restricted NKT cells may not exist in guinea pigs. These and other significant differences in the organization and function of the immune system between humans and rodents often make it difficult to translate the results obtained from rodent models to humans. Further, certain human pathogens, such as HIV-1, exhibit highly limited host selectivity, and are unable to infect into rodents and other commonly used laboratory animals.

Recently, the value of non-human primates as a model of human infectious diseases has been appreciated greatly for elucidating pathogenesis and for developing vaccines and therapies against microbial infections, such as AIDS and tuberculosis [7,8]. Nevertheless, little has been defined about the genes, proteins, and function of the group 1 CD1 molecules in non-human primates, and therefore, the present study was aimed at identifying the rhesus macaque group 1 CD1 system. We found it highly comparable to that in humans, and rhesus macaque CD1b molecules were indeed able to present a human CD1b-presented mycobacterial glycolipid Ag to specific human T cells.

* Corresponding authors. Fax: +81 75 752 3232 (M. Sugita), +81 75 761 9335 (T. Igarashi).
E-mail addresses: tigarash@virus.kyoto-u.ac.jp (T. Igarashi), msugita@virus.kyoto-u.ac.jp (M. Sugita).

0006-291X/$ - see front matter © 2008 Elsevier Inc. All rights reserved.
doi:10.1016/j.bbrc.2008.10.075

Materials and methods

Isolation of rhesus macaque group 1 CD1 cDNAs. Rhesus monkeys (*Macaca mulatta*) were used in accordance with the institutional regulations approved by the Committee for Experimental Use of Nonhuman Primates of the Institute for Virus Research, Kyoto University, Kyoto, Japan. Total RNA was extracted from rhesus macaque lymph nodes using the RNeasy mini kit (Qiagen, Hilden, Germany), and the first-strand cDNA was synthesized from 0.5 mg of the total RNA using oligo(dT) and PrimeScript reverse transcriptase (Takara Bio, Inc., Otsu, Japan). To amplify specific transcripts, the samples were subjected to PCR amplification with *Pfu* DNA polymerase (Stratagene, La Jolla, CA) for 35 cycles of 30 s at 94 °C, 1 min at 55 °C (for *CD1A*) or 60 °C (for *CD1B* and *CD1C*), 2 min at 72 °C, and a final cycle of 10 min at 72 °C. The primers used were: 5′-GCG GTA CCA AAT AAC ATC TGC AAA TGA C-3′ (sense) and 5′-GCC TCG AGA AGG AGG ATC ATG GTG TAT C-3′ (anti-sense) for *CD1A*; 5′-GCG GTA CCA GTA AGA AGT TGC ATC TCC C -3′ (sense) and 5′-GCC TCG AGG GAG CAG ACA TGG TGA GGG C-3′ (anti-sense) for *CD1B*; 5′-GCG GGT ACC ACC ATG CTG TTT CTG CAG TTT-3′ (sense) and 5′-GCG GCG GCC GCA TTG TAC TAG GCT CCT GG-3′ (anti-sense) for *CD1C*. The PCR products were purified and cloned into pcDNA3.1(+) (Invitrogen, Carlsbad, CA), and DNA sequencing was done in both directions. This procedure was repeated twice to confirm that no PCR-associated errors were introduced.

Transfection. A rhesus macaque kidney epithelial cell line, LLC-MK2 [9], was obtained from ATCC (Manassas, VA). The cells were transfected with pcDNA3.1(+) containing either rhesus macaque *CD1A*, *CD1B*, or *CD1C* by a calcium phosphate precipitation method, using the mammalian transfection kit (Stratagene). The transfected cells were then cultured in DMEM media (Invitrogen) supplemented with 10% fetal calf serum (Hyclone, Logan, UT) and G418 (0.5 mg/ml) (Invitrogen), and the CD1-expressing cells were then enriched by labeling with specific antibodies (Abs), followed by positive selection with magnetic beads coated with goat anti-mouse IgG Abs (Invitrogen). A human lymphoblastoid cell line, T2 [10], was transfected with pCEP4 (Invitrogen) containing *CD1A* or *CD1B* of either human or rhesus macaque origin by electroporation as described [11], followed by selection in RPMI1640 media (Invitrogen) containing 0.2 mg/ml hygromycin B (Invitrogen). A human cervical epithelial cell line, HeLa [12], was transfected with rhesus macaque *CD1C* in pcDNA3.1(+) by a calcium phosphate precipitation method, and selection was performed as described above. These stably transfected cells were used as Ag-presenting cells (APCs) in T cell transfectants stimulation assays.

Flow cytometry. The expression of CD1 proteins on the surface of the LLC-MK2 cell transfectants as well as rhesus macaque thymocytes were analyzed by flow cytometry as described [13,14], using the BD FACSCanto II flow cytometer. The mouse monoclonal Abs (mAbs) used were 10H3 (anti-human CD1a) [15], SN13 (anti-human CD1b) (Ancell, Bayport, MN), M241 (anti-human CD1c) (Ancell), and SP34 (anti-monkey CD3) (BD Biosciences, Franklin Lakes, NJ). MAbs MOPC-31C (BD Biosciences) and RPC5.4 (ATCC) were used as negative controls.

T cell transfectants stimulation assays. TCR-deficient Jurkat cells, J.RT3, reconstituted with either the dideoxymycobactin-specific, CD1a-restricted TCR (J.RT3/CD8-2), the glucose monomycolate (GMM)-specific, CD1b-restricted TCR (J.RT3/LDN5) or the mannosyl phosphomycoketide-specific, CD1c-restricted TCR (J.RT3/CD8-1) have been described previously [16]. The TCR-reconstituted cells (5×10^4/well) were cultured with irradiated APCs expressing a relevant CD1 isoform (1×10^5/well) in wells of 96-well, flat-bottomed microtiter plates (200 μl media/well) in the presence of 10 ng/ml phorbol myristate acetate (PMA) (Sigma, St. Louis, MO) and either the organic extract of *Mycobacterium tuberculosis* H37Ra (for J.RT3/CD8-2 and J.RT3/CD8-1) or *Rhodococcus equi* GMM (for J.RT3/LDN5) at indicated concentrations. After 20 h, aliquots of the culture supernatants were collected, and the amount of interleukin-2 (IL-2) released into the supernatants was measured by the IL-2 ELISA kit (BD Biosciences).

Molecular modeling of rhesus macaque CD1b proteins. Molecular modeling of the rhesus macaque CD1b molecule was performed, using the homology modeling software PDFAMS (Protein Discovery Full Automatic Modeling System; In-Silico Sciences, Inc., Tokyo, Japan) as described [17]. Briefly, the primary sequence of the rhesus macaque CD1b molecule was aligned with the sequence of the human CD1b molecule available from the Protein Data Bank (1UQS), using RPS-BLAST. Amino acid residues differing between the two molecules were mutated, and the obtained 3-dimensional structure was optimized by the simulated annealing method. Subsequently, the molecular model was subjected to energy minimization, using the SYBYL software. The overall structure and the cavity surface of the modeled rhesus macaque CD1b molecule were depicted in association with GMM from *Nocardia farcinica* by utilizing the MOLCAD module of SYBYL.

Results and discussion

Identification of rhesus macaque group 1 CD1 cDNAs

To isolate full-length cDNAs encoding rhesus macaque CD1a and CD1b, the first strand cDNA was synthesized from lymph node total RNA by reverse transcription, and then, PCR was carried out with specific pairs of 5′-end and 3′-end primers that were designed based on the rhesus macaque genomic *CD1A* and *CD1B* sequences. The rhesus macaque genomic *CD1C* sequence was only partially available, and the 3′-end sequence was undermined. Therefore, rhesus macaque *CD1C* cDNA was amplified by PCR using a specific 5′-end primer and a 3′-end primer that was designed based on the sequence of 3′-untranslated region of the human *CD1C* genome. The PCR products thus obtained were of expected size (approximately 1 kb) and the identity of the products was determined by DNA sequences. Identical nucleotide sequences were obtained after two independent PCR amplifications, ruling out the possibility for PCR-associated errors.

Alignment of the deduced amino acid sequences of the putative rhesus macaque *CD1A*, *CD1B*, and *CD1C* genes with the corresponding human CD1 proteins revealed a high-degree homology between the two species (85.6% for CD1a, 94.6% for CD1b, 90.4% for CD1c) (Fig. 1). The cysteine residues (indicated with triangles) involved in the intrachain disulfide bond formation in the α2 and the α3 domains as well as the putative N-linked glycosylation sites (indicated with asterisks) in the α1 and the α2 domains were totally conserved [2]. Further, the cytoplasmic tyrosine-based motif (YXXZ where Y is tyrosine, X is any amino acid, and Z is a hydrophobic amino acid) and its flanking sequences that are known to regulate differential early endosomal and lysosomal trafficking of CD1b and CD1c proteins [12,18,19] were identical between the two species (Fig. 1).

To monitor protein expression of these rhesus macaque *CD1* genes, we first screened mAbs against human CD1 proteins for their cross-reactivity to rhesus macaque thymocytes, a cell type that is presumed to express all forms of group 1 CD1 molecules. As shown in Fig. 2A, mAb clones 10H3 (anti-human CD1a), SN13 (anti-human CD1b), and M241 (anti-human CD1c) labeled a significant fraction of $CD3^{dim}$ thymocytes in a pattern comparable to that for human thymocytes [20]. We then stably transfected each